Selenology Today

Selenology Today is devoted to the publication of contributions in the field of lunar studies.

Manuscripts reporting the results of new research concerning the astronomy, geology, physics, chemistry and other scientific aspects of Earth's Moon are welcome.

Selenology Today publishes papers devoted exclusively to the Moon.

Reviews, historical papers and manuscripts describing observing or spacecraft instrumentation are considered.

The Selenology Today

Editorial Office

selenology_today@christian-woehler.de

SELENOLOGY TODAY #8
October 2007

Geological Lunar Researches Group

Cover : Image taken by George Tarsoudis

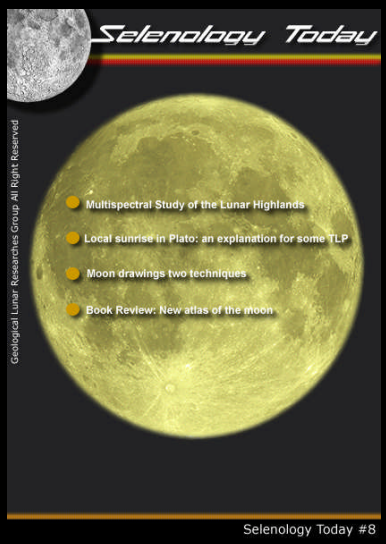

Selenology Today websites

http://digilander.libero.it/glrgroup/

http://www.selenologytoday.com/

Multispectral Study of the Lunar Highlands Adjacent to the Hypatia Peninsula from 500 nm to 1500 nm

Richard Evans
Geological Lunar Research (GLR) Group

Abstract

The lunar highlands adjacent to the Hypatia Peninsula include the Descartes and Cayley Plains areas and encompass the craters Theophilus, Dionysius, Godin and Abulfeda. This region was imaged through a small telescope using 50 narrowband filters covering the spectral range from 500 to 1000 nm, in 10 nm increments. Subsequent imaging was also performed using a short wave infrared camera and 23 additional filters covering the range from 990 nm to 1500 nm. Spectral images from both data sets were co-registered and calibrated against the Apollo 16 landing site. The image sets were then separately imported into the freeware program TNTmips lite (http://www.microimages.com/tntlite/) where they were converted into separate image hypercubes for spectral analysis. Spectra obtained for selected lunar features from each data set were merged to produce relative reflectance vs wavelength plots from 500 nm to 1500 nm. Mafic trough parameters were calculated following spline smoothing of the data and continuum line division.
The purpose of the analysis was to compare the trough characteristics to Clementine color albedo images (which assign 1000 nm Clementine images to the Red channel, 900 nm images to the Green and 415 nm images to the blue channel) and to compare results with Clementine five spectral band data. Although the spatial resolution was much inferior to that obtained by Clementine, it was anticipated that the increased spectral resolution might provide additional useful information.

Brief Primer on the Stratigraphy of the Descartes and Cayley Plains Region

In 1974, James Head wrote a seminal paper on the stratigraphy of this region. He concluded that stratigraphy here was determined more by multiple local impact events rather than by the Imbrium impacts. Probably the earliest feature in the Descartes area is a degraded unnamed 150 km diameter crater surrounding the Apollo 16 site. Nectaris Basin ejecta later formed the Descartes Mountains which were then altered by an impact forming an unnamed 60 km diameter crater centered 25 km west of the Apollo 16 site. The Apollo 16 site is located on the backslope of the uplifed outer ring of the Nectaris Basin with the uplift in this area forming the Kant plateau. Just east of this plateau, the terrain is determined by impacts creating Theophilus and Cyrillus. The flat highland area encompassing Delambre and Cayley and extending to the Kant Plateau and the Descartes Mountains is known as the Cayley Plains formation. Although various theories have been advanced to explain the Cayley Plains formation including emplacement of

ejecta from the Orientale Basin impact, it is perhaps more likely that the formation is related to multiple ancient regional crater impacts. Much more detail regarding the stratigraphy of this region can be found in Head's paper. The mafic composition of specific features in the region has been studied and areas exposed by more recent crater impacts are typical highland materials dominated by mixtures of low calcium pyroxene (norite) and anorthosite. Dionysius is known to have some superficial deposits of mare basalt focally in its rim wall and this material is found in some of its rays as well (Giguere et al., 2005). Similarly, Clementine color albedo images of Torricelli C appear to show similar deposits in the crater wall. Only a few areas of nearly pure (i.e. greater than 90 per cent) anorthosite are known and these include the central peak of Cyrillus, portions of the east rim wall of Kant and portions of the central peaks of Theophilus (Hawke et al., 1995).

Introduction

Many lunar mafic minerals can be tentatively identified via remote sensing by analysis of the reflectance spectrum obtained between about 890 and 1200 nm. The presence of a reflectance trough in this region is indicative of the presence of mafic materials containing Fe^{+2} and the depth of the trough indicates the relative amount of such materials that are present. The wavelength of the trough center assists in determining which mafic mineral is likely present. Trough centers below 950 nm are generally indicative of a low calcium pyroxene such as orthopyroxene. Examples are norite or anorthositic norite. Trough centers between 950 and 1000 nm are generally indicative of high calcium pyroxene such as clinopyroxene, which is often a constituent of gabbro. Olivine typically has a band center above 1000 nm, but may be suspected by an unusually broad trough extending through 1000 nm. Anorthosite does not show a reflectance trough between 890 and 1200 nm. Mature lunar soils, which are largely composed of regolith containing micrometeorite agglutinates, typically show only a very weak mafic signature due to the conversion of Fe^{+2} to Fe with increasing maturity. However, lunar surfaces freshly exposed by more recent cratering often show exposed mafic materials previously covered by mature regolith. These mafic materials may be seen in crater rays and in various locations within craters. Rays closer to the crater originate from greater depth in the pre-impact target site than rays that are further away. Materials composing crater walls originate from a shallower depth than crater central peaks. It is therefore possible to make some assessment of the stratigraphy of the lunar crust by analysis the mineral composition of crater features and crater rays. Tompkins and Pieters (1997) provide an excellent description of the interpretation of mineral composition from the characteristics of Clementine five band spectral plots of reflectance vs wavelength. It is possible to make an assessment of mafic composition using Clementine five filter Vis/NIR data (calibrated Clementine images are available for 415, 750, 900, 950 and 1000 nm). This can be done by plotting

spectral curves for these wavelengths as well as by examining ratio images which enhance mafic composition. Five band Clementine images in 16 bit tiff format can be downloaded from the USGS Map-a-Planet website (http://pdsmaps.wr.usgs.gov/PDS/public/explorer/html/moonpick.htm). These images are calibrated according to the method of Pieters (Pieters, 1999). Note that jpg images on this website should not be used to produce spectral plots and are only suitable for mapping purposes. Although only a handful of wavelengths are available for study, the spatial resolution of these Clementine images is excellent. Spectral studies of the lunar surface conducted through amateur telescopes can be performed at a higher spectral resolution, but are unlikely to equal the spatial resolution of Clementine images. Even so, amateur studies can be useful to the extent that a greater number of wavelength images can result in a more precise characterization of mafic troughs.

Images of a particular lunar region using a large number of interference filters can be analyzed using hyperspectral analysis software such as TNTmips lite. This software is capable of generating spectra and continuum removed spectra for every pixel imaged across the interference filter set. This spectral data can be used to conduct a detailed analysis of absorption trough areas, and depths. Spectral matching can be performed to identify mafic mineral characteristics in lunar features by virtue of this absorption trough morphology. Such studies can be further supplemented by reflectance data for individual lunar features obtained using an amateur slit/grating spectroscope (Evans, 2007) and on-line 120 color spectroscopic data obtained using the Keck telescope (http://pds-geosciences.wustl.edu/missions/lunarspec/).

Method

Multispectral images of the region of the lunar highlands surrounding the Hypatia Peninsula (between approximately 8 to 26 degrees east longitude and between 0 and 18 degrees south latitude) were obtained on April 1, 2007 between 00:00-02:00 UT. The lunar disc was 97.4 percent illuminated and the phase angle was 18.8 degrees. Images were obtained at prime focus using a 9.25 inch (23.5 cm) F10 Schmidt Cassegrain telescope.

The image scale was approximately 1.26 km/pixel. Narrowband filters between 500 nm and 1000 nm in 10 nm increments were obtained from Knight Optical in the United Kingdom (http://www.knightoptical.co.uk/). Imaging was done using a Lumenera Lu-075M camera at a gamma of 1.0 and a gain of 1.5. Exposure times varied between 100 and 1200 msec depending on the filter. Tracking was done at lunar rate using a Meade LXD75 mount. A second image set was obtained on May 27, 2007 between 00:00 and 02:00 UT and covered the wavelength range between 990 nm and 1500 nm. A Goodrich SU320MX camera was used in combination with 21 additional interference filters from Knight Optical with bandwidths between 10 nm and 18 nm. From 1000 nm to 1300 nm the filters were in 20 nm increments. This second image set was obtained under a lunar phase angle of 54.7 degrees and

78.9% illumination. Although it would have been preferable to eliminate the phase variation between the two image sets, this was not possible due to weather and imaging conditions. Images within each set were converted to bmp format and co-registered using the freeware program Blink Comparator (www.crysania.co.uk/trefach/trefach.pl). The average pixel greyscale value of a 450 pixel rectangle centered on the Apollo 16 landing site (15.6 degrees longitude, -9.0 degrees latitude) was computed for each wavelength image in turn and the image was then divided by one percent of this value using the freeware program ImageJ (http://rsb.info.nih.gov/ij/).

The resulting co-registered and calibrated image sets were multiplied by Adams original diffuse directional hemispheric reflectance values of Apollo 16 soil 62231 for corresponding wavelengths (see http://pds-geosciences.wustl.edu/missions/lunarspec/). The original or wavelength corrected versions of the Adams 62231 soil reflectance data are utilized to calibrated images taken through Earth based telescopes while the bidirectional reflectance data for the 62231 soil is used in Clementine image calibration. Greyscale pixel values for the image sets were multiplied by five to achieve adequate viewer rendering of the images and then each data set was imported separately into the freeware program TNTmips lite (www.microimages.com/tntlite/) for processing into hyperspectral datacubes. This program was used because it generates spectral plots automatically and the number of wavelength bands involved was fairly large. The methods and principles of hyperspectral analysis using TNTmips lite are discussed in a set of tutorials that can be optionally downloaded with this freeware program.

The most important tutorials in this regard are hyperspec.pdf (www.microimages.com/getstart/pdf/hyprspec.pdf) and hypanly.pdf (www.microimages.com/getstart/pdf/hypanly.pdf). Hypercube creation and analysis has become the method of choice for hyperspectral image analysis by the remote sensing community. Note that for those persons who do not want to take the time to learn to use TNTlite or similar programs that create and analyze hypercubes, it is equally possible to simply use the image stack and histogram options in ImageJ to manually determine the reflectance for the desired pixel area for each wavelength bands in the program ImageJ. Spectral plots could then be produced using Excel or a similar spreadsheet. Spectra for individual pixels or pixel groups were then obtained for both image sets for areas of interest and then combined into single reflectance vs wavelength plots covering the range from 500 nm to 1500 nm. Spectra were smoothed using a 25-30% B spline in the program TableCurve2 (www.systat.com/). A continuum line was drawn tangent to the spectral curve of the feature and was defined by two points on the curve located on either side of the trough. The first point was almost always selected at 750 nm on the wavelength axis. When possible the second point was selected at 1500 nm, but in some cases it was necessary to select a point at between 1100 nm and 1300 nm on the wavelength axis to preserve

tangency. The feature spectrum was divided by the continuum line and trough parameters were calculated from the resulting reflectance vs wavelength plot. Clementine five band spectra for the lunar feature of interest were prepared by downloading 16 bit tiff images of the feature of interest from the USGS geosciences PDS node (http://pds-geosciences.wustl.edu/missions/lunarspec/index.htm). These images have already been calibrated by the method of Pieters (Pieters, 1999) but must still be multiplied by 0.000135 to achieve absolute reflectance. Only 16 bit tiff images (not the jpg images which are suitable only for mapping) should be used. Reflectance values were measured for each wavelength in ImageJ by using the image stack and histogram features. The trough morphology of the reflectance vs wavelength plot can be compared to examples provided in Tompkins and Pieters (1997) to determine which specific mafic component or mixture of components is present. This paper by Tompkins and Pieters is an invaluable resource and should be studied carefully. Figure 1 shows the lunar region imaged in the present study. Principal features are labelled since they can be more difficult to identify at full moon than when present adjacent to the lunar terminator. The region consists of the lunar highlands adjacent to the Hypatia peninsula, but adjacent mare are also included. Principal craters present in this region include Dionysius, Theophilus, Cyrillus, Abulfeda, Delambre, Agrippa, Hypatia, Torricelli C, Kant, Moltke etc.

Results

Trough parameters for many identifiable features were calculated as described above and the results tabulated. The strength of the mafic band was compared to the appearance of the Clementine color albedo image of the feature, and in some cases to 5 band Clementine reflectance vs wavelength plots. In general, trough parameters for highly anorthositic features with trough depths less than about 2.5 percent of the reflectance scale were not computed due to spectral noise.

Spectral noise was moderately accentuated near the splicing point of the two camera data. However, occasionally lower noise levels in the spectra allowed the calculation of parameters for shallow troughs, with Alfraganus C being an example. The effects of lunar phase differences between the two telescopic data sets were monitored by comparing the combined reflectance plots with the Adams directional reflectance data for the Apollo 16 site.

Phase angle differences did not produce an observable alteration in continuum slope of the combined data sets when compared to the directional reflectance data for the Apollo 16 site.

A more detailed description of selected features is provided in the following pages.

Note that all spectral plots shown in the sections which follow are shown as relative reflectance vs wavelength, except for plots showing Clementine 5 band UVVIS spectra. These Clementine UVVIS plots are shown as absolute reflectance vs wavelength.

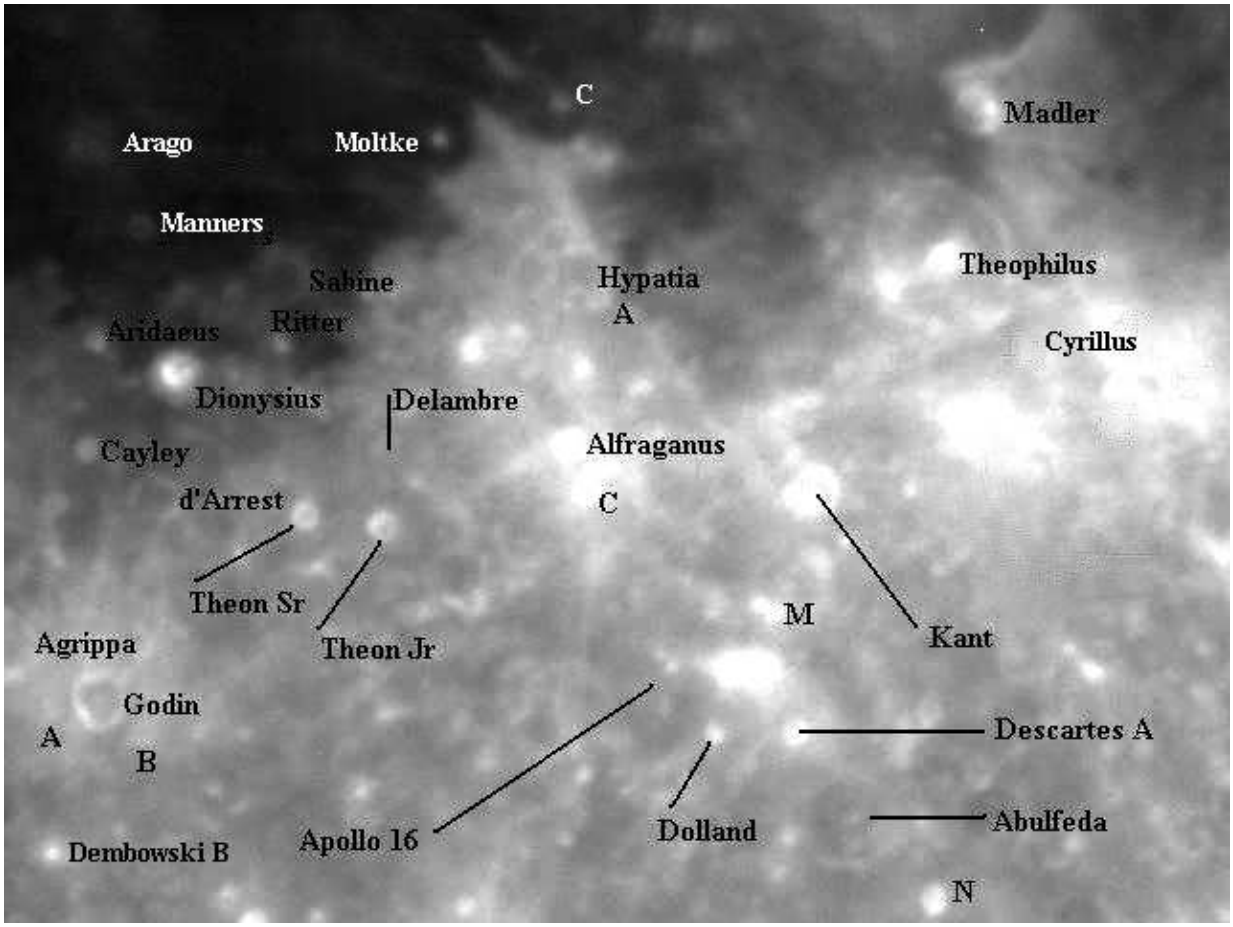
C
Madler
Arago
Moltke
Manners
Theophilus
Sabine
Hypatia
A
Ritter
Aridaeus
Cyrillus
Dionysius
Delambre
Alfraganus
Cayley
C
d'Arrest
Theon Sr
M
Kant
Agrippa
Theon Jr
Godin
A
Descartes A
B
Apollo 16
Dolland
Abulfeda
Dembowski B
N

Figure 1

A. Dionysius Crater (West Wall)

Dionysius is a 17.6 km diameter crater at the southeastern edge of Mare Tranquillitatis. This region was recently studied by Giguere et al. (2005) using Clementine images. In that study, Dionysius was felt to be primarily composed of anorthositic norite with some dark basalt deposits present fairly superficially on the eastern and southern portions of the crater wall. This basalt was felt to be an extension of the Mare Tranquillitatis basaltic flow. The west wall, however, is nearly free of basaltic material and is primarily composed of anorthositic norite. Rays nearest to Dionysius have previously been determined to be composed of anorthositic norite and are felt to have originated from ejection of the deepest crater material. Figure 2a below is a Clementine 1000 nm image while Figure 2b is a telescopic image of the crater from the present study. The dark wall deposits are basaltic while the remainder of the crater is felt to be composed of anorthositic norite. They are even better visualized in a ratio image assigning 1000 nm to the red channel, 900 nm to the green channel, and 415 nm to the blue channel as shown in Figure 3. The mafic deposits have a blue, indigo, or indigo black color.

Figure 2

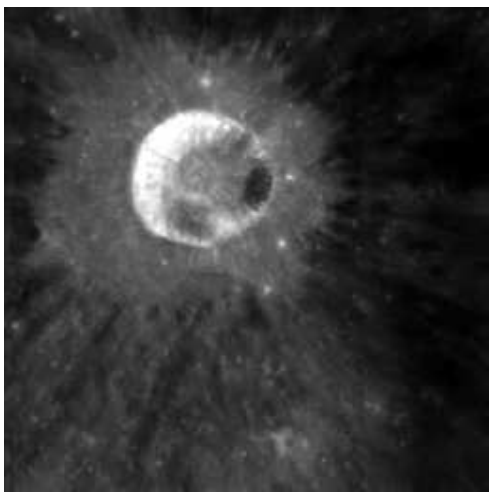

Figure 2b

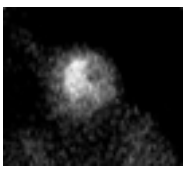

Figure 3

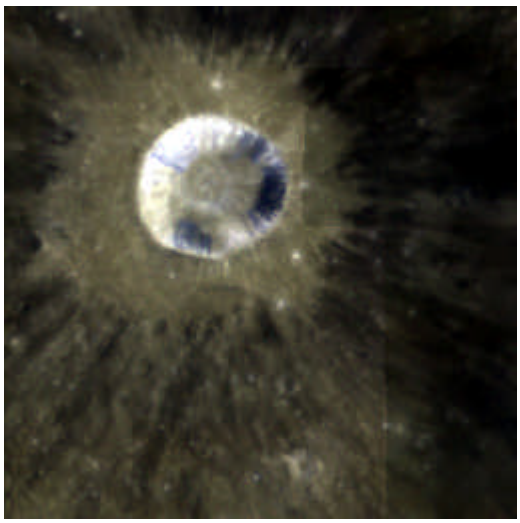

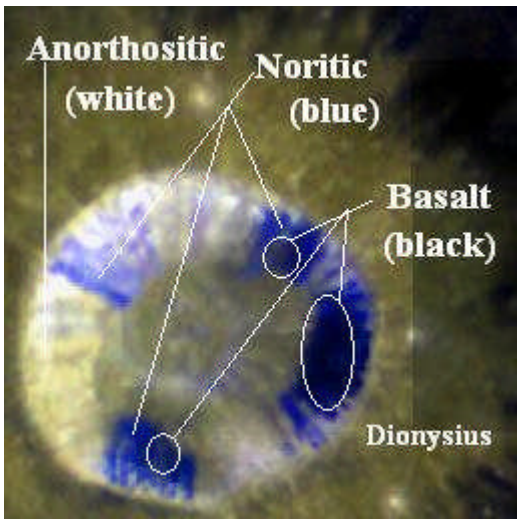

Staid and Pieters (1998) analyzed Clementine five filter spectra for Dionysius and other small craters. Figure 4 is a plot of the Clementine reflectance spectra for Dionysius which shows evidence of the basalt deposits in the east and south walls. Trough morphology for gabbroic high calcium pyroxene can be found in Tompkins and Pieters (1997) for comparison purposes. Five band spectra for various regions of the crater wall suggest the presence of areas dominated by high calcium and low calcium pyroxenes as well as mixtures of the two.

Figure 4

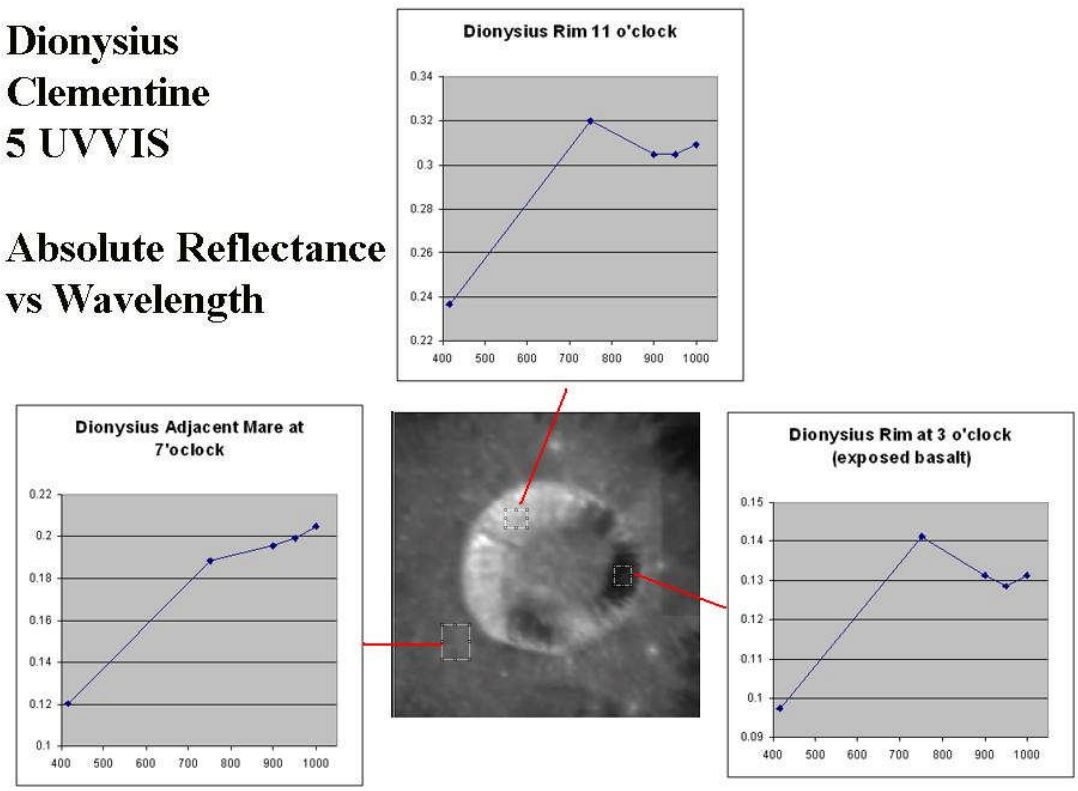

The spectral plot of the west wall of Dionysius obtained from 500 to 1300 nm in the present study is shown in Figure 5a and 5b below. The reflectance scale in Figure 5a is in relative reflectance units. The reflectance scale in Figure 5b is in absolute reflectance units where telescopic data have been re-scaled to the 750 nm Clementine absolute reflectance value. Figure 5c compares the telescopic reflectance plot with Adams Apollo 16 soil 62231 reflectance.

Figure 5a

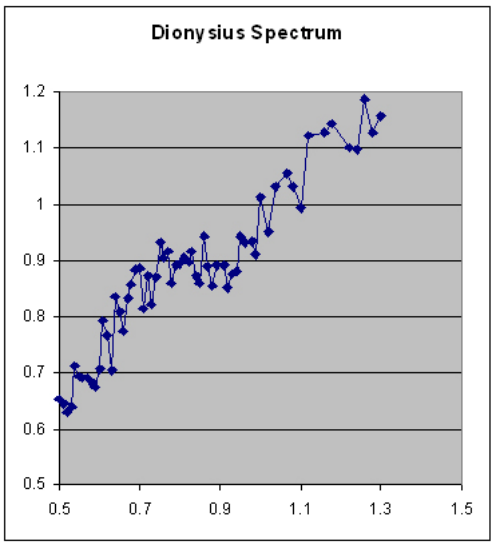

Figure 5b

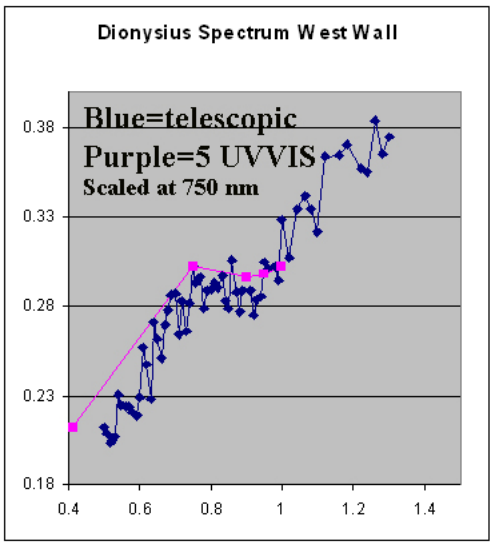

Figure 5c

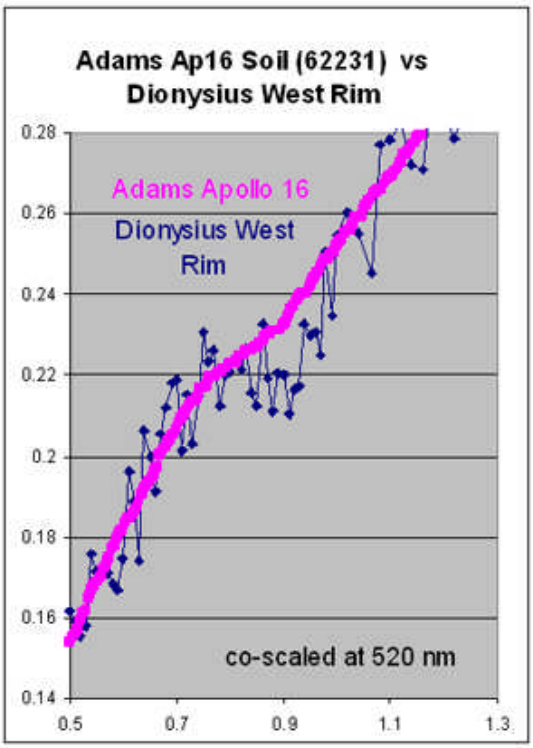

A 30% smoothing B spline was applied to this data set in TableCurve2 and a continuum line was drawn tangent to the resulting curve at 750 nm and 1153 nm. The result is shown in Figure 6 while Figure 7 provides a more detailed view of the trough area.

Figure 6

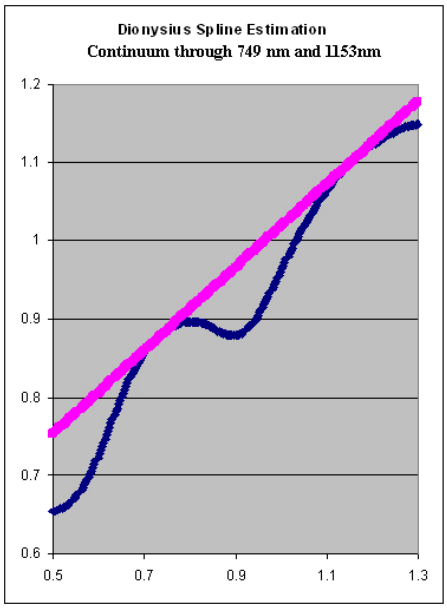

Figure 7

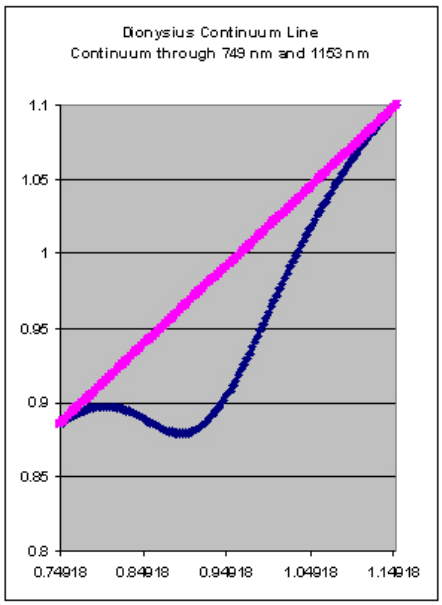

The result of division of the spectral plot (blue) by the continuum line (purple) is shown in Figures 8 and 9.

Figure 8

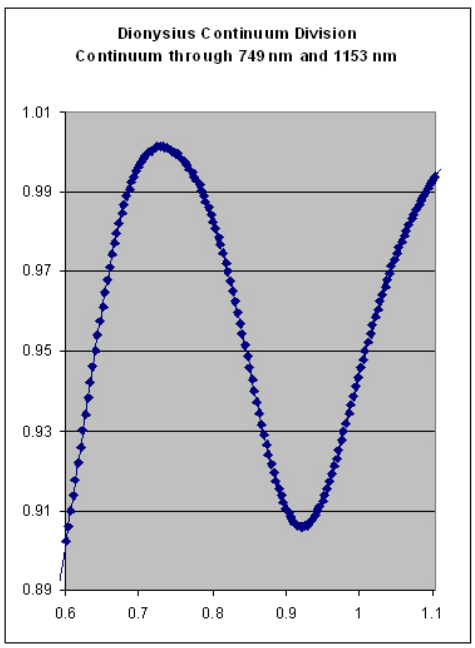

Figure 9

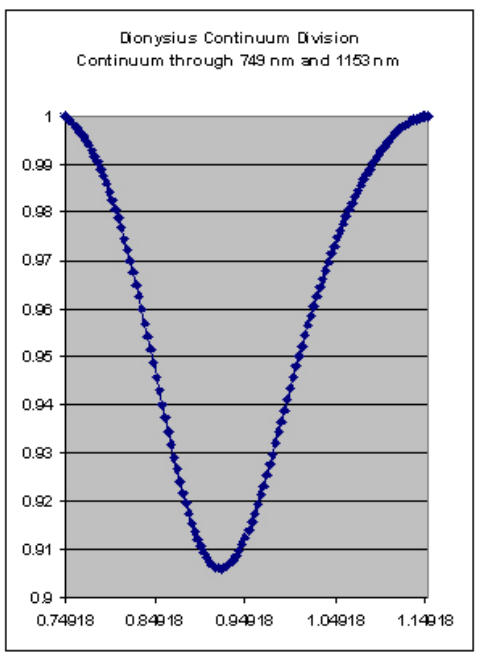

Trough parameters for Dionysius West Wall calculated from these plots are shown in the Table 1.

Table 1

Center	Half Width	Full Width	Max. Depth	Integrated Area
923 nm	174 nm	348 nm	9.4%	29 nm refl. units

Results indicate a low calcium pyroxene as the principal mafic component in the western wall of Dionysius and are consistent with anorthositic norite. There is no indication of a basaltic component in this portion of the crater wall. This is consistent with the Clementine color albedo image of Dionysius shown in Figure 3.

B. Torricelli C

Torricelli C is a small crater near the mare rim adjacent to the eastern portion of the Hypatia Peninsula and is not far from Moltke. The Clementine color albedo image of this crater is shown in Figure 10a. Dark areas in the crater wall are present nearly circumferentially and are suggestive of basalt deposits. The Clementine five band reflectance plot for the dark mafic areas in the crater wall is shown in Figure 10b. The trough morphology indicates the presence of a high calcium pyroxene component (Tompkins and Pieters, 1997).

Figure 10a

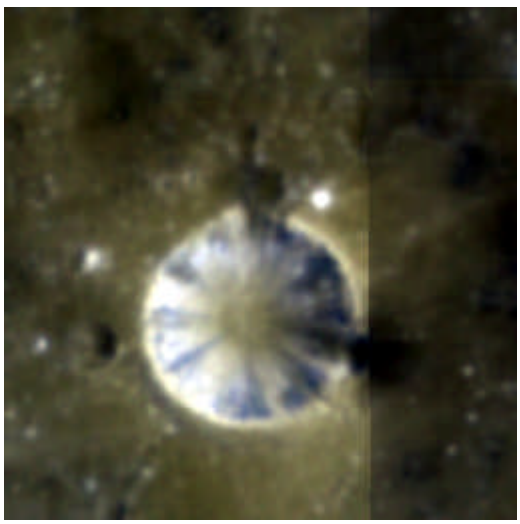

Figure 10b

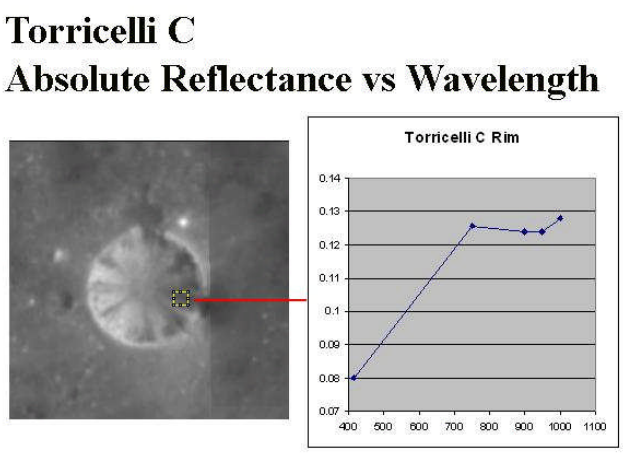

The 500-1500 nm reflectance vs wavelength plot is shown in Figure 11a and the comparison with Adams Apollo 16 soil 62231 is shown in Figure 11b.

Figure 11a

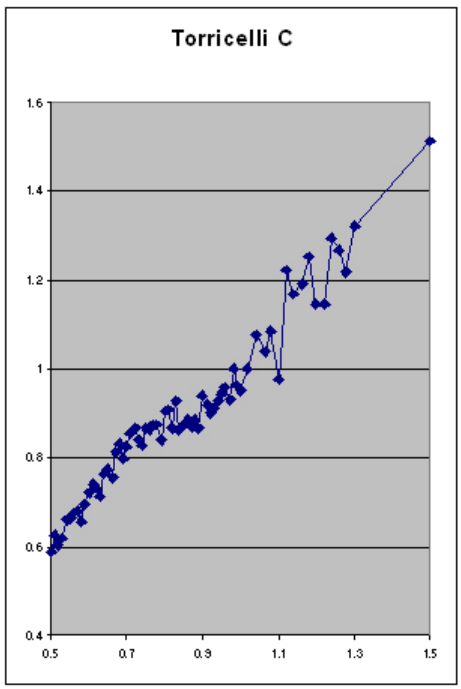

Figure 11b

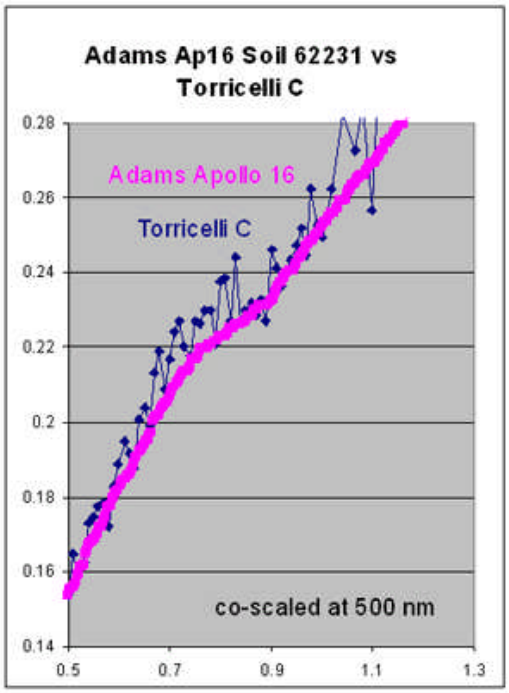

The spline smoothed result with application of a continuum line at 750 nm and 1500 nm is shown in Figure 12 with a narrower view shown in Figure 13.

Figure 12:

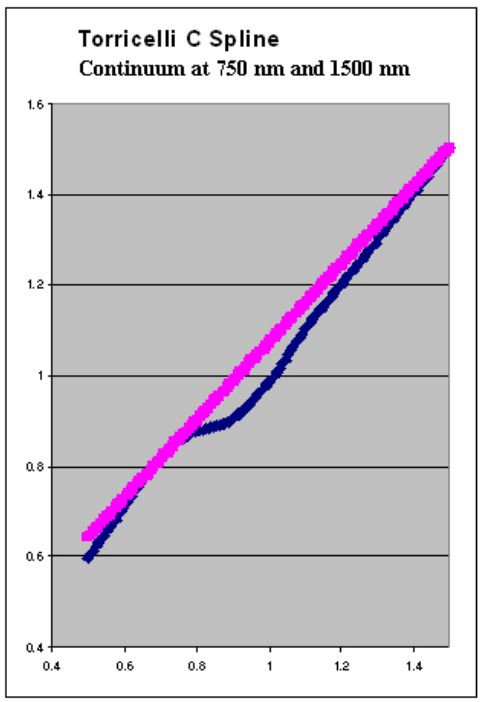

Figure 13

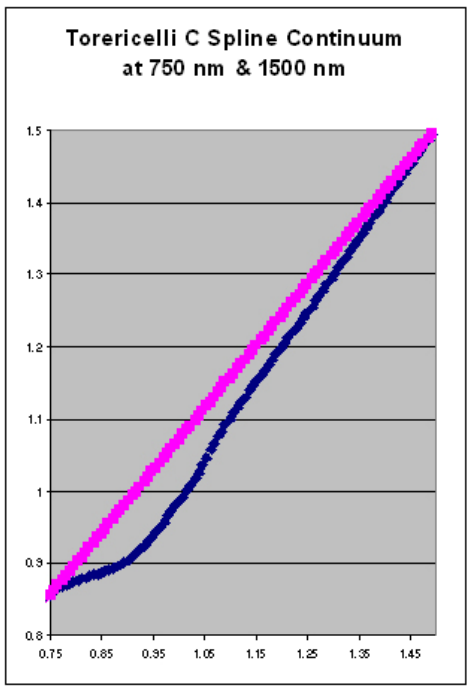

The result of division of the smoothed Torricelli C spectrum by the continuum line is shown in Figures 14.

Figure 14

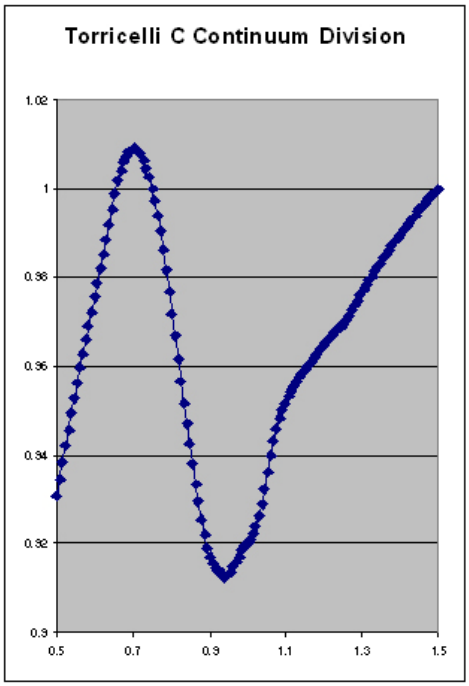

Trough parameters for Torricelli C calculated from this data are shown in Table 2.

Table 2

Center	Half Width	Full Width	Max. Depth	Integrated Area
947 nm	235 nm	470 nm	9.6%	40 nm refl. units

These parameters are consistent with a mixed low calcium and high calcium pyroxene composition for the crater walls. This likely reflects a mixture of anorthositic norite and basalt and is consistent with the initial interpretation of the Clementine color albedo image for this feature.

C. Moltke

Moltke is a 5.4 km diameter crater located near the edge of the tip of the Hypatia peninsula. It is estimated to have a depth of about 1310 meters. Figure 15 below shows the Clementine 750 nm image of Moltke.

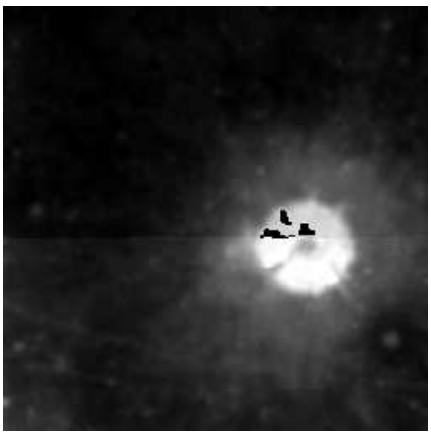

Figure 15

The several black defects in the crater image appear to be calibration artifacts. They are unfortunately much more severe in the 415 nm calibrated Clementine image, making it difficult to create useful mafic ratio images or a five band spectral plot. The Clementine color albedo image was found to be oversaturated and not useful. However, Figure 16a shows the reflectance curve for the present study and does contain useful information in spite of the lower spatial resolution. Figure 16b compares the result with Adams Apollo 16 soil 62231 reflectance.

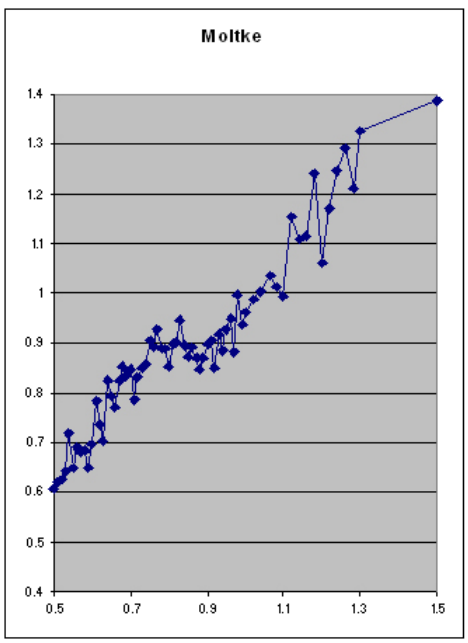

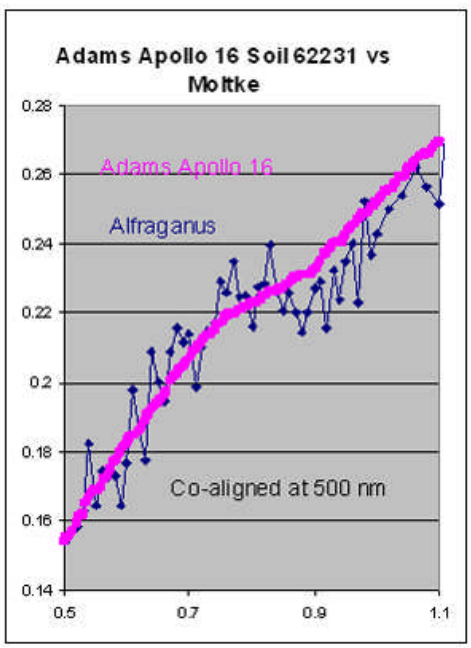

Figure 16a (left)

Figure 16b (right)

The result of spline smoothing of this data and application of a continuum line is shown in Figure 17.

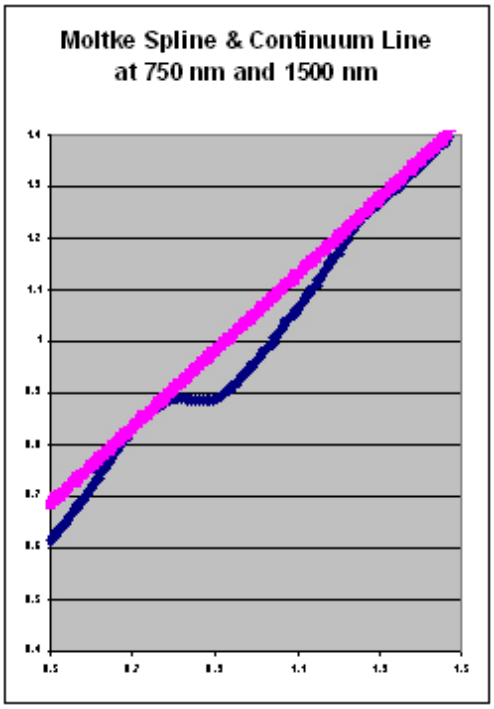

Figure 17

A plot of the continuum division is shown in Figure 18

Figure 18

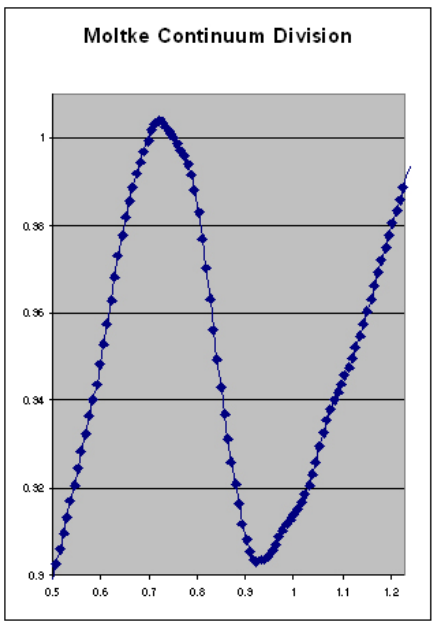

Trough parameters for Moltke calculated from this data is shown in Table 3

Table 3

Center	Half Width	Full Width	Max. Depth	Integrated Area
932 nm	212 nm	424 nm	10.0%	38 nm refl. u.

These results indicate a low calcium pyroxene composition for Moltke, consistent with anorthositic norite. There is no indication of a basaltic component.

D. Theon Senior

Theon Senior is a 18.2 kilometer which, together with Theon Junior, forms a crater pair adjacent to Delambre. The Clementine color albedo image for the pair is shown in Figure 19 (Theon Senior is above Theon Junior). Figure 20 is a closer view of Theon Senior.

Figure 19

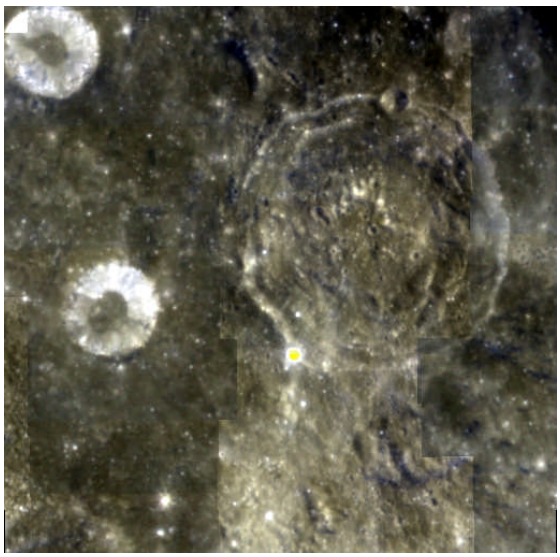

Figure 20

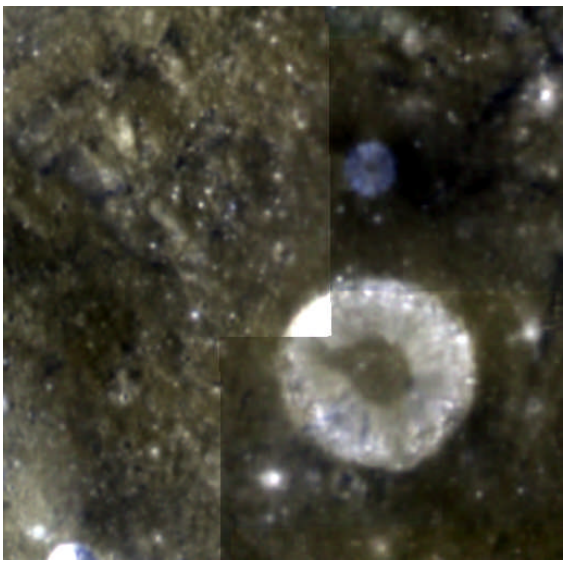

The reflectance plot from 500 nm to 1500 nm from the present study is shown and compared with the Clementine UVVIS five band specta and the Adams Apollo 16 soil 62231 in Figure 21a – 21c. The spline smoothed data with placement of a continuum line and the continuum division are shown in Figures 22 and 23 respectively. Trough parameters calculated from these plots are shown in Table 4.

Figure 21a

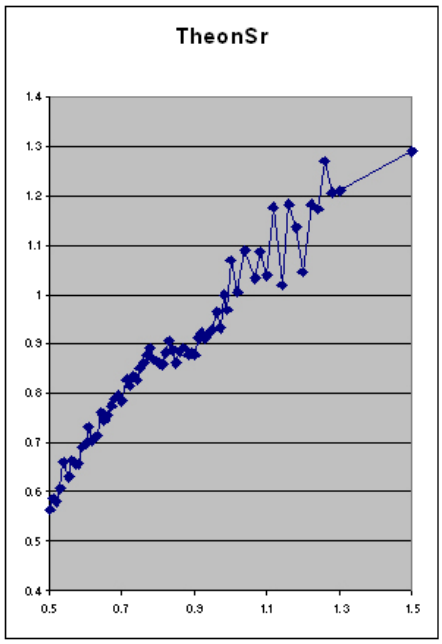

Figure 21b

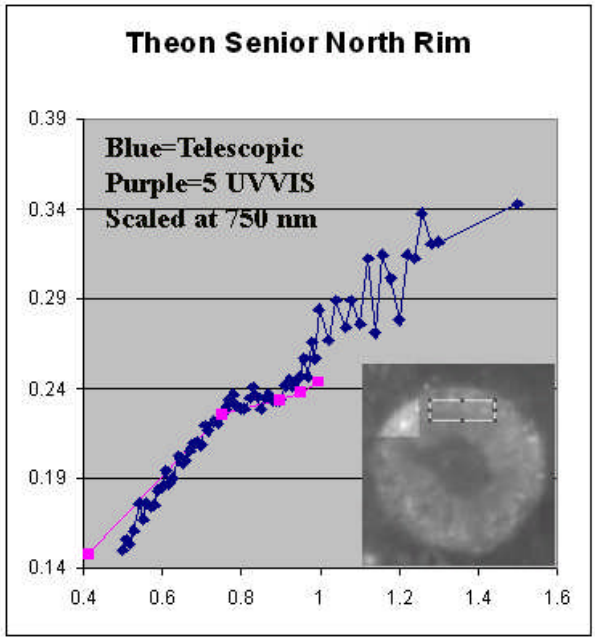

Figure 21c

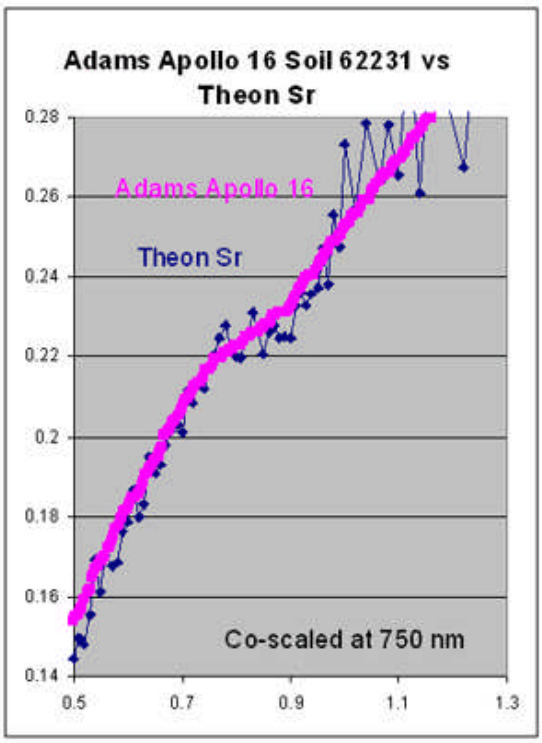

Figure 22

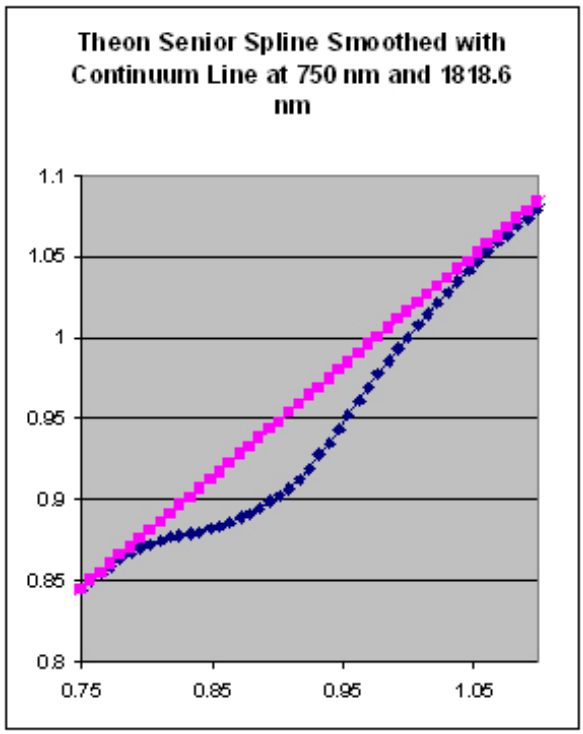

Figure 23

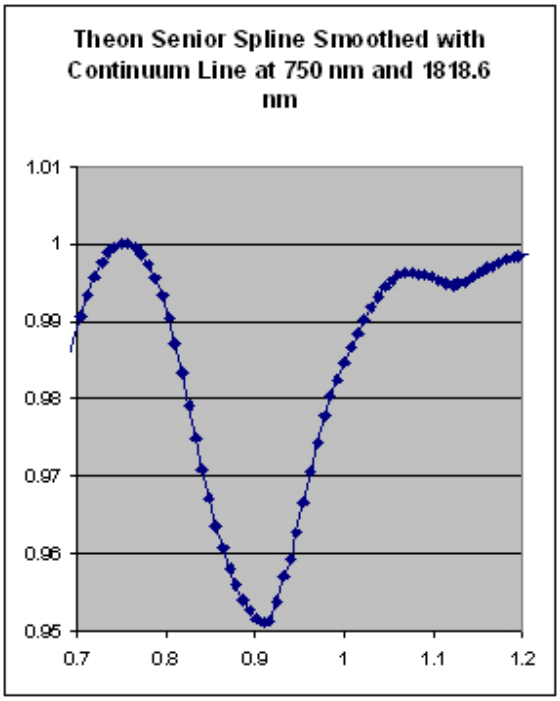

Table 4

Center	Half Width	Full Width	Max. Depth	Integrated Area
909 nm	152 nm	303 nm	4.9%	13 nm refl. u.

E. Theon Junior

Theon Junior has a diameter of 18.6 km and is the twin of Theon Senior. The pair is shown together in Figure 19. Figure 24 shows a Clementine color albedo image of Theon Junior.

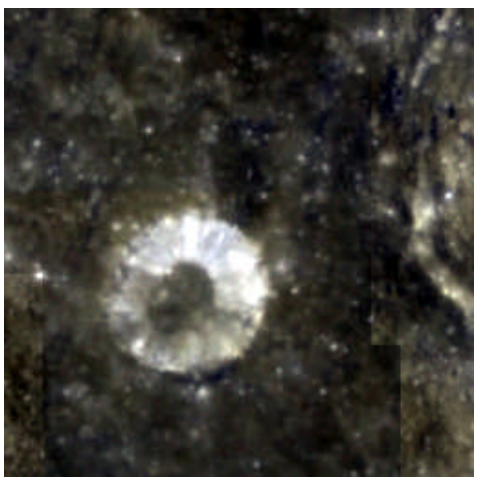

Figure 24

Figures 25a – 25c compare the telescopic reflectance plot with Clementine UVVIS five band spectra and Adams Apollo 16 soil 62231 soil reflectance. Figures 26 and 27 respectively show the 500-1500 nm spline smoothed reflectance data with continuum line placement, and the continuum division plot from the present study.

Figure 25a

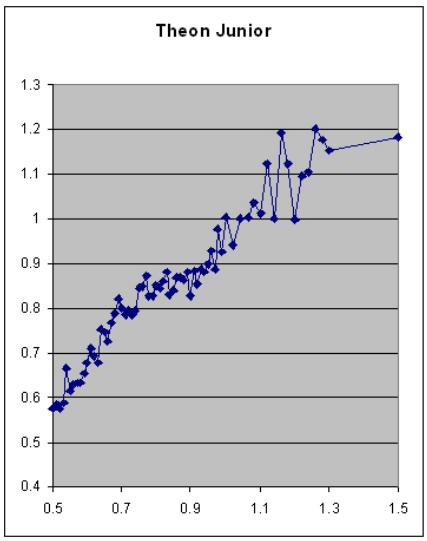

Figure 25b

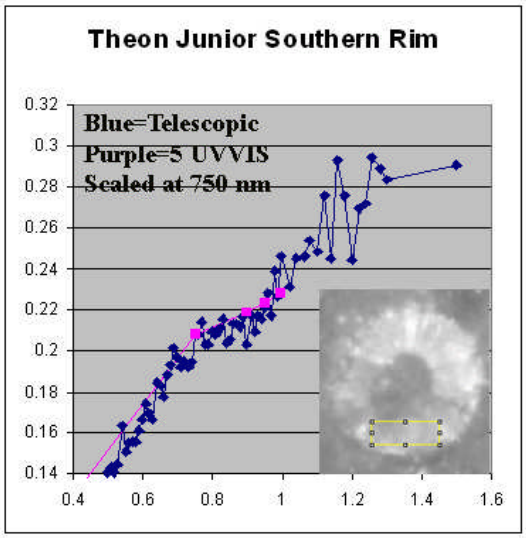

Figure 25c

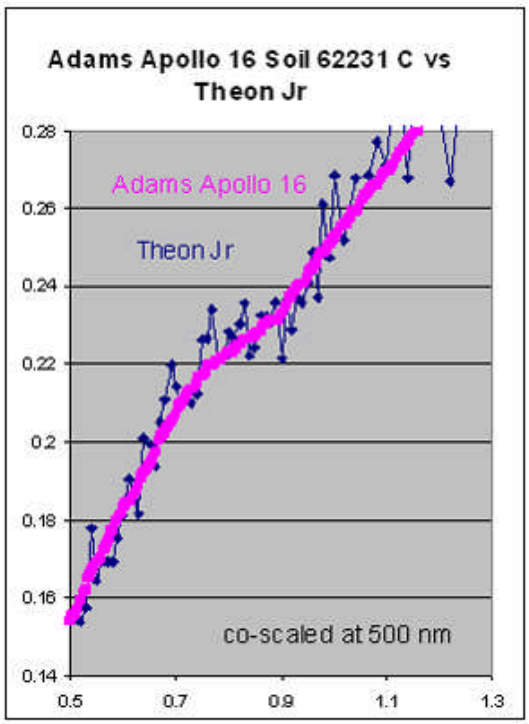

Figure 26

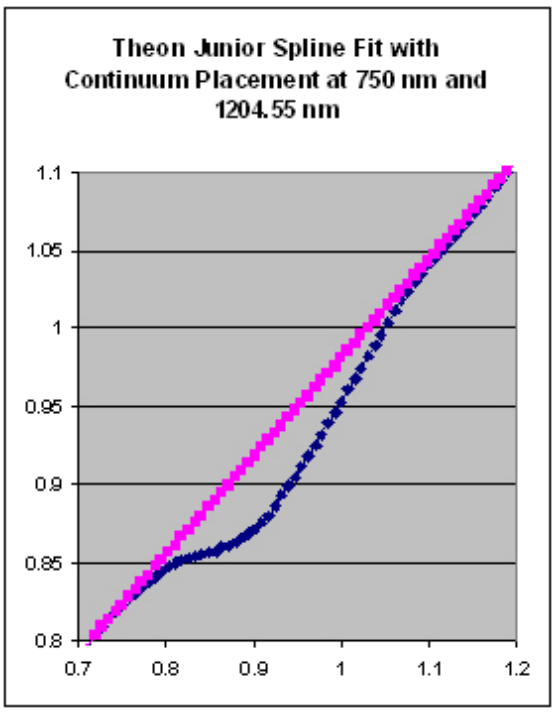

Figure 27

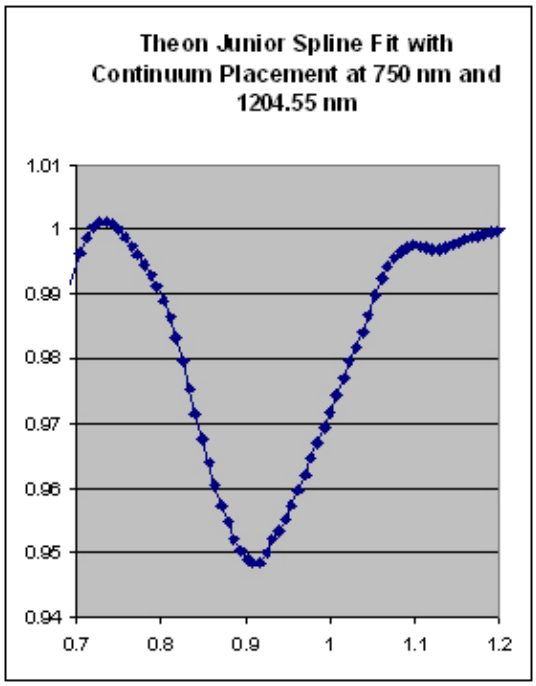

Trough parameters calculated from these plots are shown in Table 5 below.

Table 5

Center	Half Width	Full Width	Max. Depth	Integrated Area
909 nm	174 nm	349 nm	5.3%	16 nm refl. units

F. Kant Crater, North Wall

Kant crater is a very well known crater with a prominent central peak located on the Kant Plateau, adjacent to Theophilus. The USGS color albedo image shows prominent darkening of the northern portion of the rim (Figure 28a) which indicates the likely presence of mafic material. The most likely possibility is anorthositic gabbronorite (Figures 29 and 30).

Figure 28b is the 1000 nm Clementine image with the 23.5 cm telescope image from the present study inset.

Figure 28a

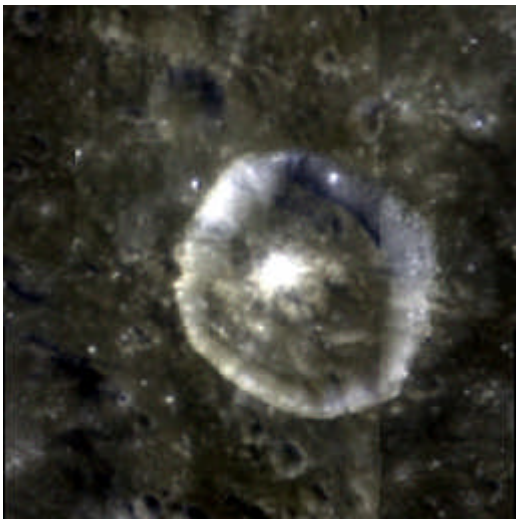

Figure 28b

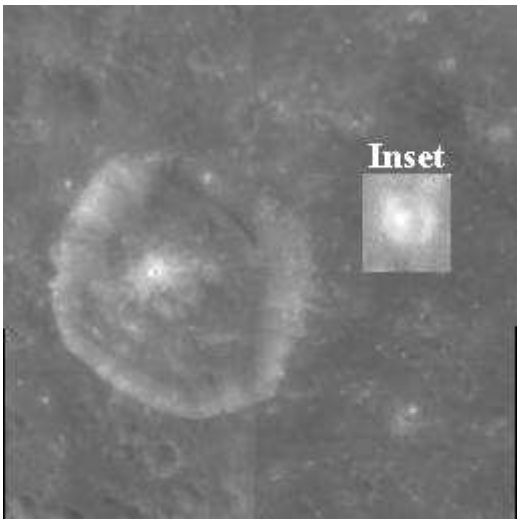

Figure 29

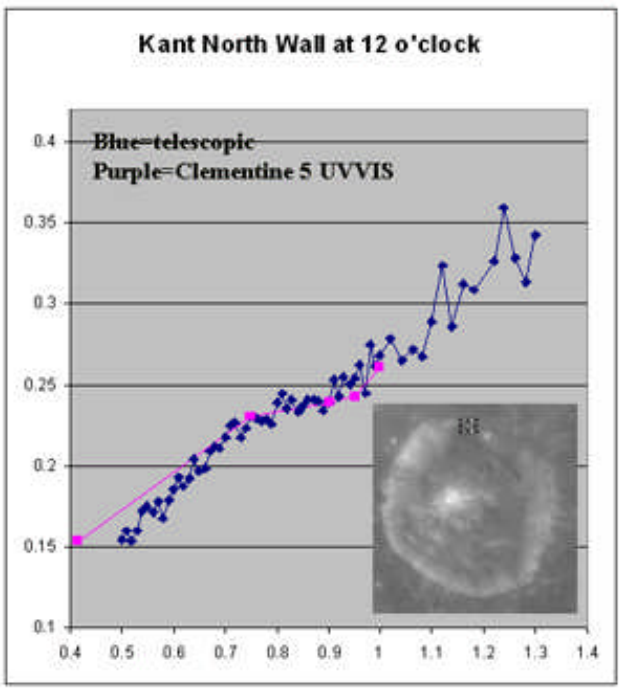

The reflectance plot from the current study is shown in Figure 30a. A comparison with the Adams Apollo 16 soil 62231 is shown in Figure 30b. The spline estimate (60 percent smoothing) with continuum line at 750 nm and 1250 nm is shown in Figure 31. The result of division by the continuum line is shown in Figure 32.

Figure 30a

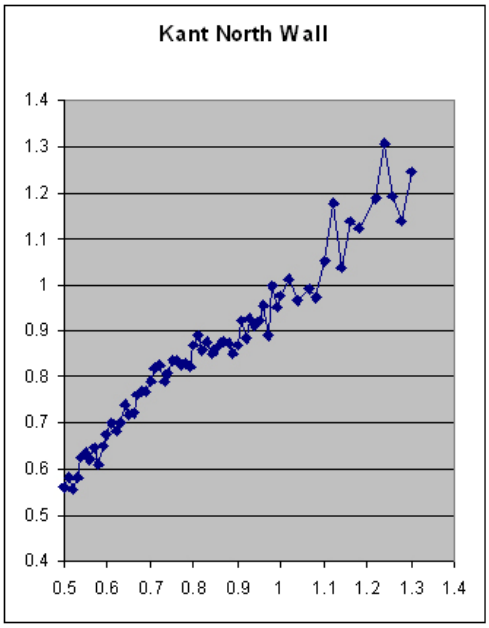

Figure 30b

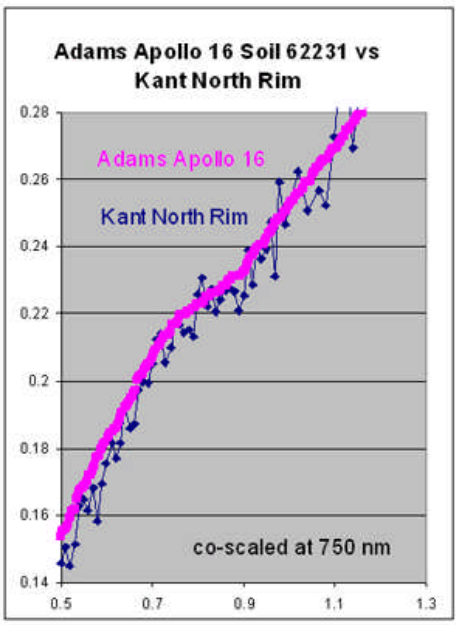

Figure 31

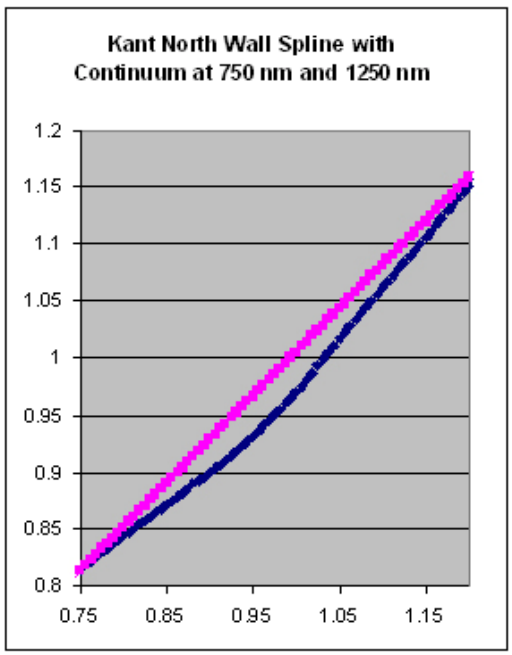

Figure 32

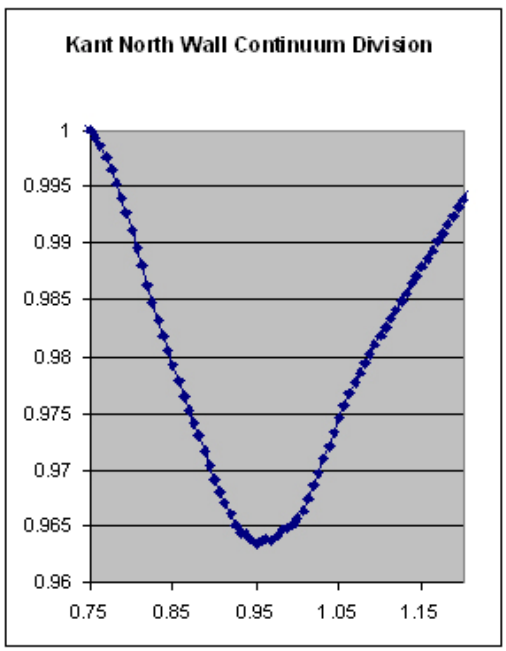

Table 6

Center	Half Width	Full Width	Max. Depth	Integrated Area
963 nm	213nm	425 nm	3.6%	14 nm refl. units

G. Alfraganus

Alfraganus is a 21 kilometer diameter crater located in the highlands just west of Sinus Asperitatis. Except for its southern portion, the rim wall has a mafic appearance on the Clementine color albedo image shown in Figure 33.

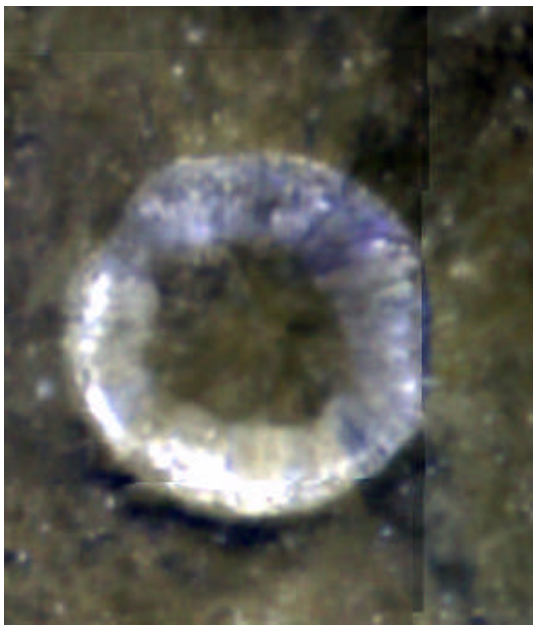

Figure 33

Clementine 5 band spectra (Figure 34) show anorthositic norite as the mafic material while the present study indicates an anorthositic gabbronorite.

Reflectance spectra from the present study are shown in Figures 35a – 35c as compared to Clementine five band spectra and Adams Apollo 16 soil 62231.

Figures 36 and 37 show spline smoothed reflectance spectra with continuum line placement and continuum line division.

Figure 34

Alfraganus
Absolute Reflectance vs Wavelength

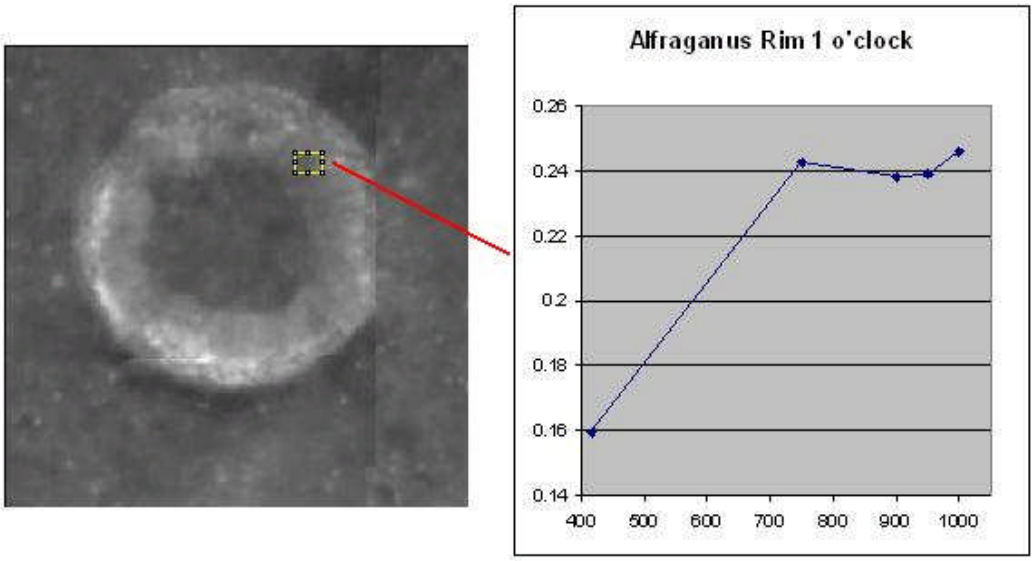

Figure 35a

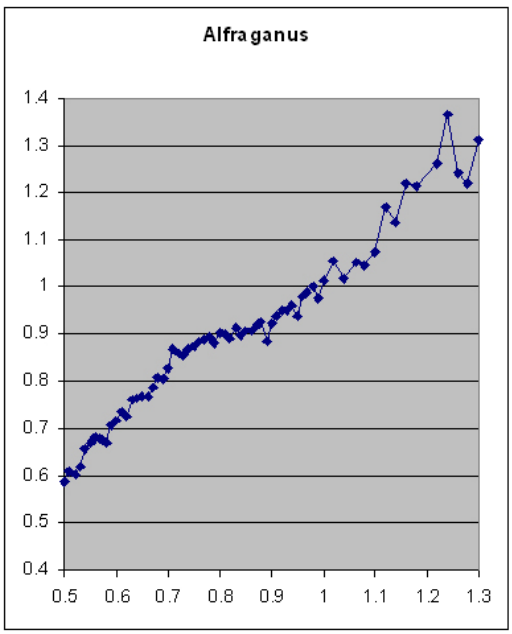

Figure 35 b

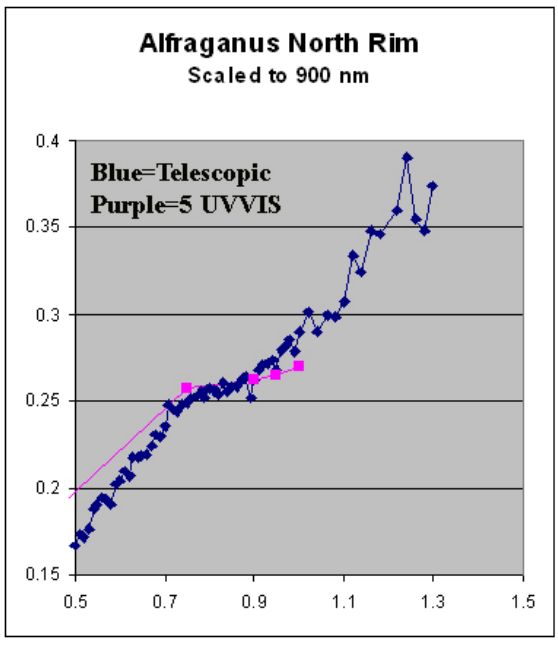

Figure 35c

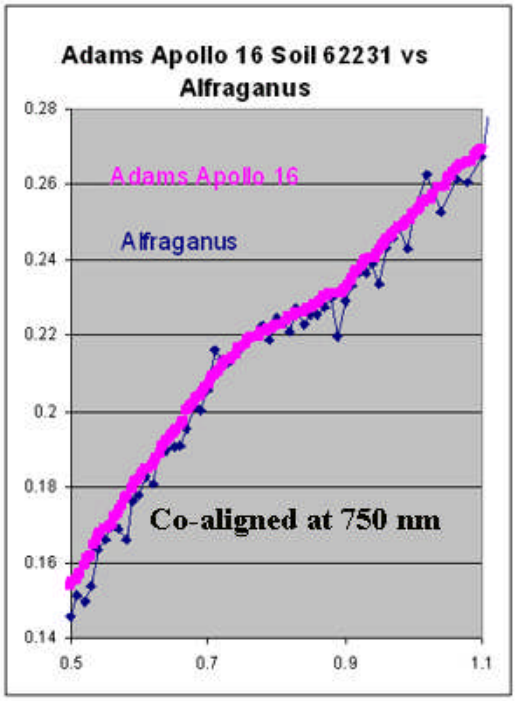

Figure 36

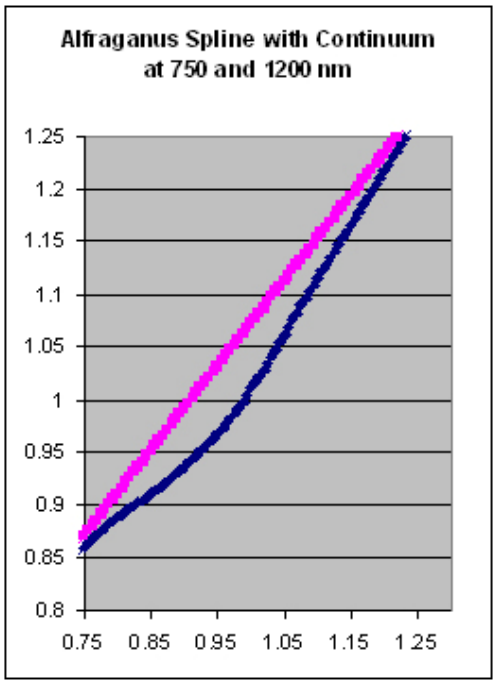

Figure 37

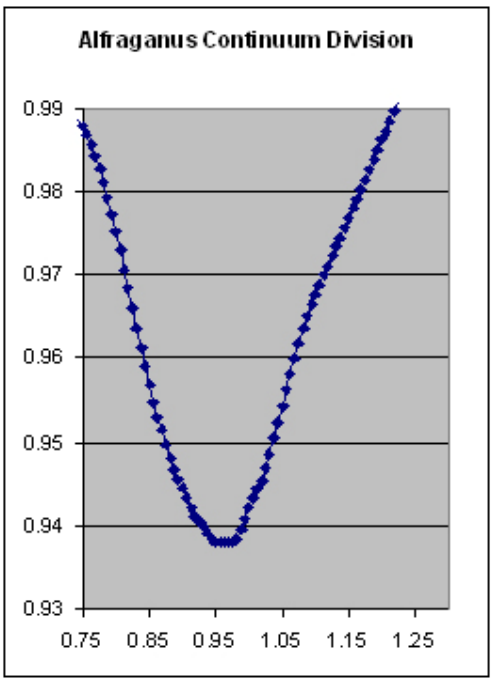

Trough parameters calculated for the north rim area of Alfraganus from the present study are shown in Table 7.

Table 7

Center	Half Width	Full Width	Max. Depth	Integrated Area
963 nm	233 nm	465 nm	5.2%	21 nm refl. units

Trough parameters for other features

Table 8

Crater	**Trough Center (nm)**	**Trough Maximum Depth in percent of reflectance scale**	**Trough Width (nm)**	**Integrated Area of Trough in nm reflectance units**
Dionysius West Rim	920	8.6	334	25
Moltke	932	8.8	288	22
Ariadaeus	919	7.2	295	19
Theophilus Peak	----------	less than 2.5%	----------	----------
Cayley	925	5.7	283	14
Alfraganus	963	5.2	465	21
Alfraganus C	915	2.2	283	6
Kant East Rim	----------	less then 2.5%	----------	----------
Madler	924	4.8	283	12
Descartes E	912	4.0	234	8
Torricelli C	947	8.7	394	30
Theon Senior	909	4.9	303	13
Theon Junior	909	5.3	349	16
Kant Peak	----------	less than 2.5 %	----------	----------
Kant North Rim	963	3.6	213	14

Summary

Detailed reflectance spectra from 500 nm to 1500 nm were obtained for the lunar highlands encompassing the Hypatia peninsula using a small telescope. The spectra were quite detailed as compared with Clementine five band spectra, but the spatial resolution was extremely modest due to the low magnification employed and the effects of the atmosphere. Features less than about 10 km in diameter were not well visualized across the full range of hypercube images. Nonetheless, there appeared to be reasonable correlation with mafic deposits suggested by Clementine color albedo images and Clementine five band spectra. Clementine spectra of mafic deposits show substantial heterogeneity for areas only a few pixels apart reflecting local differences in mafic concentrations. Telescopic spectra, due to lower spatial resolution, tend to reflect regional averages for these trough depths. If the resolution of small telescope multispectral images could be increased by imaging at a modestly higher magnification and better compensating for atmospheric effects, it is likely that spatial resolution could be further increased. If it had been possible to take the two sets of images on the same night they could have been processed into a single hypercube. This would have allowed the preparation of spectral match image maps for different trough characteristics produced in TNTmips lite. Unfortunately, preparation of spectral maps covering the complete wavelength range from 500 to 1500 nm could not be prepared from data in the present study and it remains a future goal. Spectral noise in the present data sets precluded calculation of trough parameters for most features with trough depths of less than about 2.5 percent of the reflectance scale. The present study was primarily intended as an exploration of methodology. Even so, the results support the current understanding of the general stratigraphy of this lunar region. Unfortunately it was not possible to obtain visible and NIR image sets at the same phase angle in this study. Although phase angle induced error (due to red shifting at larger phase angles) is probably quite small in this study, results should be viewed only as approximate, and are not definitive. It is encouraging, however, that the Adams Apollo 16 soil 62231 reflectance spectra compare favorably with the continuum slope of lunar features imaged in the present study. More detailed evaluation in the future will require that both sets of images be taken at the same phase angle, preferably during the same imaging session. In conclusion, this study demonstrates the feasibiltiy of using a small telescope (together with visible and near infrared cameras and a set of interference filters) to develop multispectral data sets for hypercube generation. Software such as TNTmips lite enables the generation of spectra from such image sets which can then be used to further analyze absorption trough characteristics using programs such as EXCEL and TableCurve2. The general methodology for such procedures is explained in the text of the paper.

Calibrated Clementine NIR images are available on the USGS website (see http://astrogeology.usgs.gov/Projects/ClementineNIR/). Currently these are only available at lower resolution and

only in ISIS (Integrated Software for Imagers and Spectrometers) cube format. ISIS software capable of reading and analyzing the cubes is available for download from the USGS website but can only be used on Linux systems see (isis.astrogeology.usgs.gov/nstallation/index.html).

At some point in the future, this data will also become available on the USGS map-a-planet website.

One direction for future work in the area of amateur lunar spectroscopy would involve adding Clementine NIR data from 1100 nm to 2650 nm to analyses using 5 UVVIS data discussed in this paper.

It is likely that the combination of these two data sets would allow trough centers to be better characterized and compared to results of amateur telescopic studies.

References

[1] Blewett DT, Hawke DR, Lucey PG (2001) Reflectance Spectra of Lunar Pure Anorthosites and of Mercury. Lunar and Planetary Institute Conference. Mercury: Space Environment, Surface and Interior. Abstract #8013.

[2] Charette MP, Taylor ST, Adams JB, McCord TB (1977) The detection of soils of Fra Mauro basalt and anorthositic gabbro in the lunar highlands by remote spectral reflectance techniques. Proc. Lunar. Sci. Conf. 8th p. 1049-1061.

[3] Evans, RJ (2007) Analysis of Lunar Spectra and Multiband Images. Selenology Today. Issue #7 pp. 1-46.

[4] Giguere TA, Hawke BR, Gaddis LR et al. (2005) "Remote Sensing Studies of the Dionysius Region of the Moon". Lunar and Planetary Science XXXVI, abstract #1092.

[5] Hawke BR, Taylor GJ, Lucey GJ et al. (1995). Remote Sensing Studies of Anorthosite Deposits on the Moon. Meteoritics Vol. 30 No. 5 p. 518.

[6] Head, James (1974) Stratigraphy of the Descartes Region (Apollo 16): Implications for the origin of samples. The Moon. vol. 11, pp. 77-99.

[7] McCord TB, Grabow M, Feierberg MA, MacLaskey D and Pieters CM (1979). "Lunar multispectral maps: Part II of the lunar nearside." Icarus 37: 1-28.

[8] Pieters CM and Tompkins S. (1999) The distribution of lunar olivine/ troctolite outcrops: Mineralogical evidence for mantle overturn? Lunar Planetary Science XXX abstract #1286.

[9] Pieters CM (1999) The moon as a spectral calibration standard enabled by lunar samples.
The Clementine example. Workshop on new views of the moon2: Understanding the moon through the integration of diverse datasets. Flagstaff, Az. abstract #8025.

[10] Staid M, Pieters CM (1998) "A Re-evaluation of Lunar Basalt Types Through Spectral Analysis of Fresh Mare Craters" Lunar and Planetary Science XXIX abstract #1853

[11] Tompkins, S and Pieters CM (1997) Composition of the lunar crust beneath megaregolith. Lunar and Planetary Science XXVIII #1251.

Local lunar sunrise in Plato- an explanation for some TLP

By Raffaello Lena, Jim Phillips, Maria Teresa Bregante and Piergiovanni Salimbeni

Geologic Lunar Research (GLR) group

Abstract

The nature and reality of transient lunar phenomena (TLP) is still an open problem for the professional lunar science community. We show that an observational Transient Lunar Phenomenon (TLP) report concerning a Plato observation by Kelsey on 18 April 1967 (entry #1027 in the Cameron catalog) is not a TLP but the normal appearance of this crater.

1. Introduction: overview about the TLP catalogs

A transient lunar phenomenon (TLP) refers to short-lived lights, colors, or changes in appearance of the lunar surface. TLPs have been reported for centuries, but their nature is largely unsettled, and even their existence as a coherent phenomenon is still controversial. Recently, Crotts (2007a-d) has conducted statistical studies of the events reported in two TLP catalogs published by Cameron and Middlehurst (Cameron 1978, 2006; Middlehurst 1968; 1977). The purpose of these catalogs is to provide a listing of historical and modern records that may be useful in investigations of possible "activity on the moon". Crotts links the locations of TLPs with moonquakes and radon gas emissions detected by Apollo and Lunar Prospector (2007b-d) suggesting that escaping gases might explosively loft a cloud of regolith above the surface, creating the temporary change of a TLP. There is no commonly accepted physical explanation for TLPs, and some authors even question if they are due to processes local to the Moon at all. Cameron (1972) divides TLPs into four categories: “brightenings” white or color-neutral increases in surface brightness, “reddish” red, orange or brown color changes with or without brightening, “bluish” green, blue or violet color changes with or without brightening, and “gaseous” obscuration, misty or darkening changes in surface appearance. Middlehurst et al. (1968) compiled a catalog of all known changes reported on the Moon. These were historical accounts of flashes, clouds and obscuration. Each entry includes a brief description and date of the observation, the name of the observer(s) and the reference.

The Cameron catalog includes all reported TLP regardless of the perceived weight of the observation (Cameron, 1978). A wide overview about the TLP, observations and methods, is also published by Crotts (2007a, and references therein). Several programs, primarily by groups of amateur astronomers, but sometimes involving professional researchers, have made organized observations of the Moon.

These projects have been organized with the ALPO (Association of Lunar

and Planetary Observers, (http://www.lpl.arizona.edu/rhill/alpo/lunar.html see also http://www.ltpresearch.org/), the BAA (British Astronomical Association, http://www.britastro.org/baa/, see also http://www.cs.nott.ac.uk/acc/) and GLR group (http://www.glrgroup.org/). Although the nature and reality of TLP is still an open problem for the professional lunar science community, some surveys carried out by the GLR group have explained some classic TLP observations as events due to viewing geometry (Lena and Cook, 2004). Lena and Cook (2004) discussed a couple of past TLP observations concerning an Alphonsus observation by Poppendiek and Bond on 19 November 1958, and a Ptolemaeus observation by Bartlett on 3 November 1973, reporting that two events (entries #705 and #1380 in the Cameron catalog) are not TLP but normal appearances of these craters. It is supported by the recurrence of brightness as seen in observations made under the same specific lighting conditions of events described as TLP.

Amongst the many lunar sites where visual observers claimed to have recorded anomalies, Plato is one of the best known with 114 TLP events (Cameron, 1978). In the past Plato has been the focus of controversy over several suspected lunar changes, including luminous milky kind of light (entries #229 by Williams, #209 by Klein, #403 by Goddard in the catalog). Streaks and the presence of points of light have been observed by P. Fauth (Middlehurst et al., 1968, http://www.mufor.org/tlp/1890.html) and also by J. Schröter (1791). Entry #1027 in the Cameron catalog concerns an event recorded on Plato by Kelsey on 18 April 1967 at 03:10-04:00 UTC from Riverside (California), using a 20 cm Newtonian telescope, 300x magnification. The observer reported: “Streak on Plato’s floor showed slight enhancement in red filter compared to blue filter. Later, a second streak formed. Probably the Sun shining thru a valley in the rim. Red enhancement permanent”. The Plato event was assigned a weight of 3 in the catalog (Cameron, 1978), which indicates: a single observation, “probably a good observer”. A systematic investigation of a large set of observations during local lunar sunrise/sunset has not been undertaken so far. We studied Plato using observations made under illumination conditions that matched the event described by Kelsey, illustrating the shape and the appearance of the observed streaks. We show that also this event described by Kelsey (Cameron, 1978) is not a TLP but a normal appearance of this crater.

2. Historical background: drawings and observations

Historical observations and drawings of Plato with streaks on the floor have been reported also by simultaneous but geographically well-separated observers (Crotts, 2007a). Crotts (2007a) reports 2 simultaneous observation of the same event recorded on May 2, 1895 for 12-14 min on the floor of crater Plato (see also Middlehurst et all http://www.mufor.org/tlp/lunar.html and references therein): Brenner observed a streak of light, while Fauth, independently, reported bright, parallel bands with a his drawing shown in Fig. 1.

Johann Schröter drew the identical phenomenon (Fig.2) and reproduced it in his lunar classic *Selenotopographische Fragmente* (1791). Adams noted on two occasions near sunrise, when the interior of Plato was filled with shadow, that two beams of light traversed two-thirds of the floor resembling searchlights; they were parallel and well defined, and had "the appearance of passing through a slight vapour resting on the surface" (Webb, 1962). Streaks on the Plato's floor were also reported by North (12 February 1981 at 20:56 UT). This appearance, reported by other observers from time to time (see Fig. 3), is particularly interesting: the streaks appear to touch, extending gradually to the west wall which is very odd, as the floor convexity should prevent this (Marshall & Mobberley, 1986).

Furthermore, Robinson (http://www.lunar-occultations.com/rlo/rays/plato.htm) describes a similar observation carried out by Kingsley (June 8, 2003) as the appearance of a Plato "sunrise ray". It seems the presence of spots of light and streaks on the Plato's floor at sunrise has been described and known for a very long time. We have organized several observations of Plato in order to determine if the "sighting" reported under entry #1027 in the Cameron catalog is a transient event, or if it was just the natural appearance of the lunar site given the local lighting conditions at that phase of the lunation. These observations will be described in detail in Section 5.

3. Topographic and geologic settings of Plato

Plato is centered at latitude 51.60° north and 9.30° west and has been the subject of numerous TLP reports and topographic studies principally because of its dark floor and large size. In addition Plato has a number of interesting craterlets on the floor (for their description see also http://www.space.edu/moon/other/plato/PlatoChanges.html). Moreover, Marshall & Mobberley (1986) describe the possibility that the central craterlet is situated on top of a pressure bulge which slopes downwards to the north at this point. Plato is located on the border of Mare Imbrium and Montes Alpes. To the west the crater is situated Bliss (formerly Plato A), named on various early maps as Jackson-Gwilt (Marshall & Mobberley, 1986). The irregular Mare Frigoris is located to the north. The Lunar Orbiter IV image shows what appears to be considerable subsidence just inside the crater walls, especially to the northwest and southeast wall, there emerges a rift tangential to the wall. To the northeast of the crater lies a rille (part of Rimae Plato) which originates near crater Plato G and travels to Mare Frigoris. When seen from Earth, Plato is subject to foreshortening in the north-south direction, giving it a noticeably elliptical aspect. Plato is a walled plain 101 km in diameter (Pike, 1976). It is interesting to note that Plato has no central peak. Compared to the other craters of similar size, Plato should have a 2.2 km high central peak rising from its floor (Wood, 1973). However since Plato is filled with lava the peak may be buried. Another feature worth noting is the absence of floor fracturing. On the western wall there is a large massif disconnected from the crater rim; this

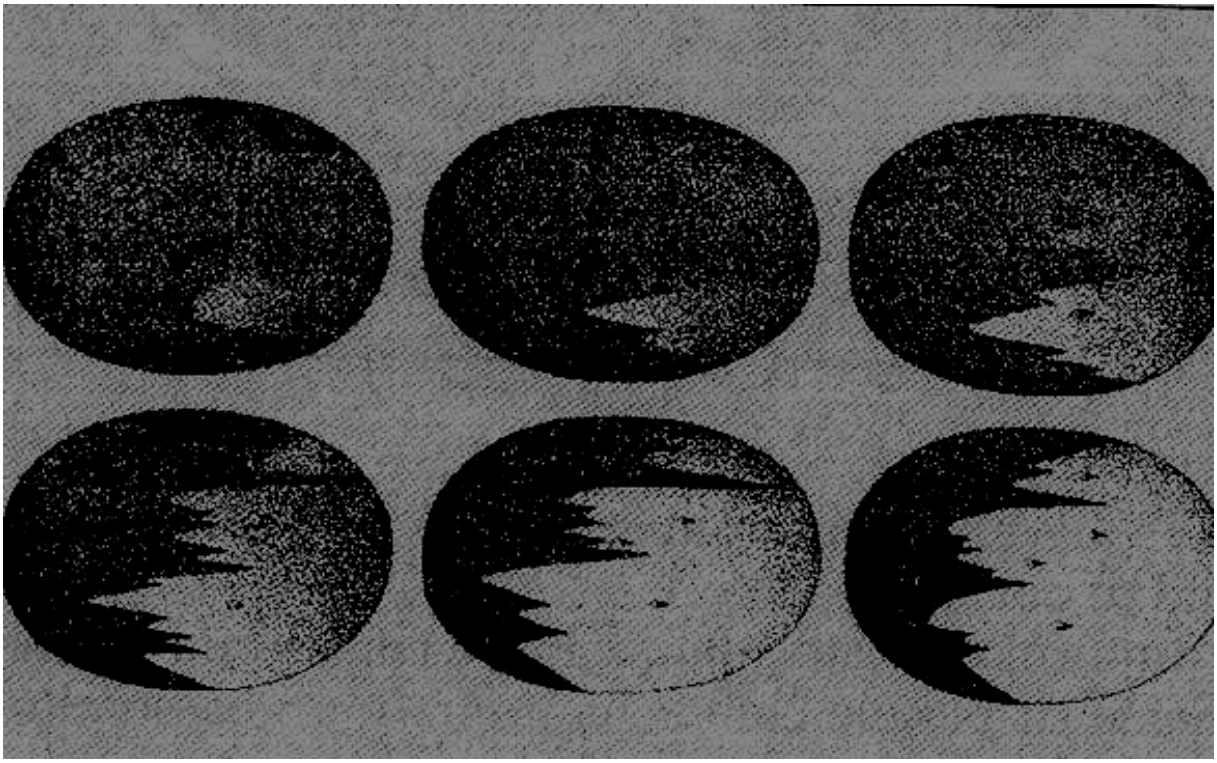

Fig. 1: Drawing by Fauth, local sunrise in Plato.

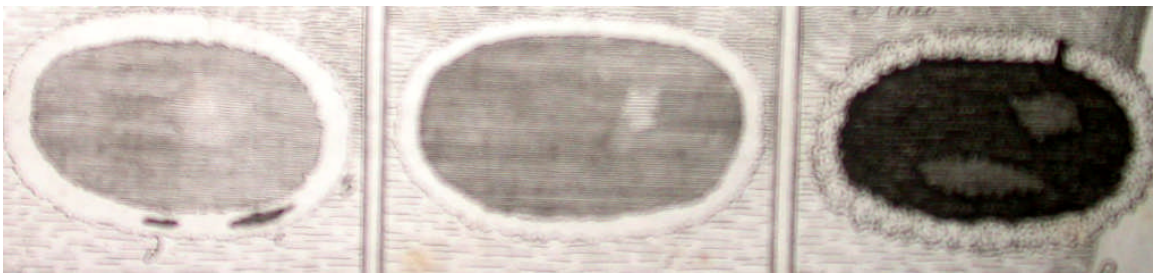

Fig. 2: Drawing by Schröter (1791), local sunrise in Plato.

massif resulted from giant landslides. Plato was formed after the Imbrium impact but before the lava flooding that formed Mare Imbrium. A geologic interpretation about the single units is given in the USGS I-701 map, Geologic Atlas of the Moon Plato quadrangle (M'Gonigle & Schleicher, 1972 and references therein). The lava that filled Plato is likely younger than the lava in the nearby Mare Imbrium; in fact there are fewer small impact craters on Plato's floor than would be expected if it were the same age as the mare (M'Gonigle & Schleicher, 1972). The western and north western rims contain various dark albedo features which form quite intricate patterns. Three main rays (although even these are elusive) and many subtle ones crossing the region are described (Marshall & Mobberley, 1986). As far as the albedo variations on Plato's floor are concerned, there appears to be a connection between the markings on the southwest floor and the nearby rays crossing the crater and the mare Imbrium to the south. In particular, one ray, which appears to travel well beyond the mountain Pico beta, and travels past the north-west edge of Pico itself, occasionally appears to cross the floor of Plato (Marshall & Mobberley, 1986). Marshall & Mobberley (1986) examine this ray and the two other bright rays, which may originate from the crater Anaxagoras. Moreover, under favourable illumination the ray in question appears to line up exactly with the eastern edge of the floor region.

4. Material and measurements: observations which match the lighting conditions for the April 1967 Plato event #1027

Table 1 lists the 6 observers who supplied a total of 12 observations. For each of the observations, the local lunar altitude of the Sun (α), the azimuth of the Sun (Az), the Sun's selenographic colongitude (Col) and the Sun's latitude were calculated using the Lunar Observer's Tool kit by H. D. Jamieson (1992). The "Sun's selenographic colongitude" is the longitude of the morning terminator. By using this software we computed (assuming for the reproducibility of the event the central coordinates of Plato, longitude -9.3° latitude +51.6°) dates and times when the lighting conditions closely matched those for the illumination origin of the TLP event reported for Plato (#1027); these are reported in Table 2. The observation carried out on May, 9, 2003 closely matched the condition of Kelsey's observation, also for the value of the libration and the Sun's latitude. All the images used for this study are shown with south at the top and west to the right (see figures 3-7). The height measurements were computed using the LTVT software package by Mosher and Bondo (2006) which requires a calibration of the images by identifying the precise selenographic coordinates of some landmarks on the image. This calibration was performed based on the UCLN 1994 list of control points. The computed values were obtained with the shadow length mode, based on the sun angle α at a peak and the angular distance from the peak to the tip of the shadow. The software computes the difference in elevation between the point at the tip of the shadow and the point on the raised lunar feature casting the shadow. We will discuss these results in the section 6 and 7.

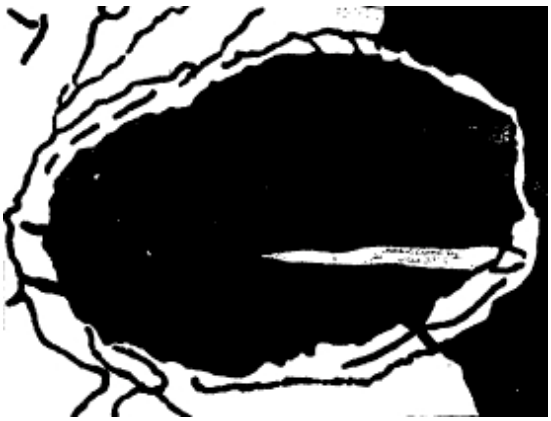

Fig. 3: Drawing by North on February 12, 1981 at 20:56 UT. Courtesy of BAA.

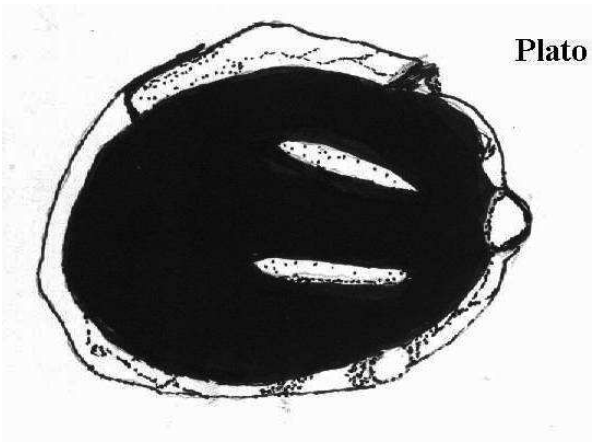

Fig. 4a: Drawing by Lena on May 9, 2003 at 18:25 UT

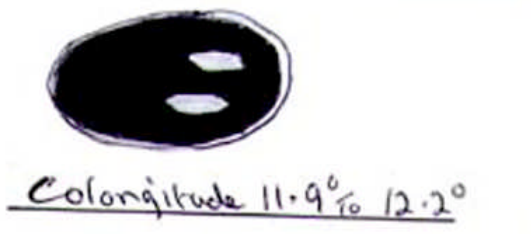

Fig. 4b: Drawing by Marie C. Cook on May 9, 2003 at 20:00-20:30 UT, see also www.cs.nott.ac.uk/~acc/Lunar/2003may.htm

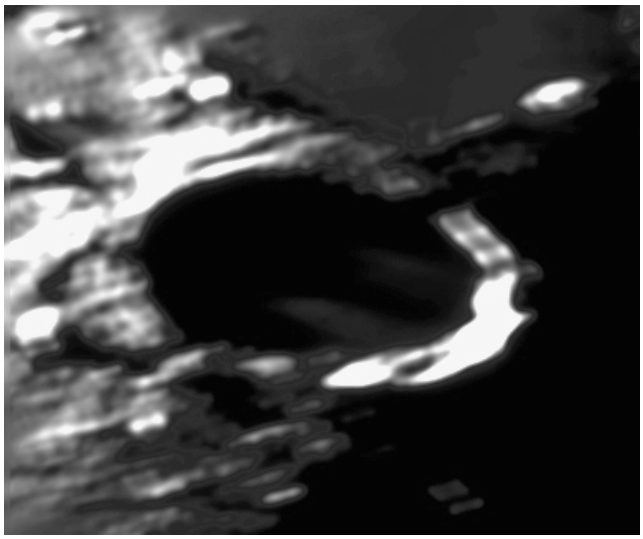

Fig. 5a: Plato streaks as imaged by Phillips on March 19, 2005 at 02:17 UT

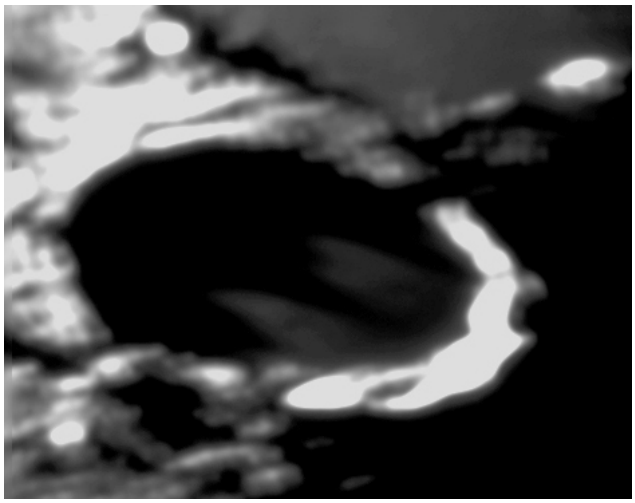

Fig. 5b: Plato streaks as imaged by Phillips on March 19, 2005 at 02:58 UT

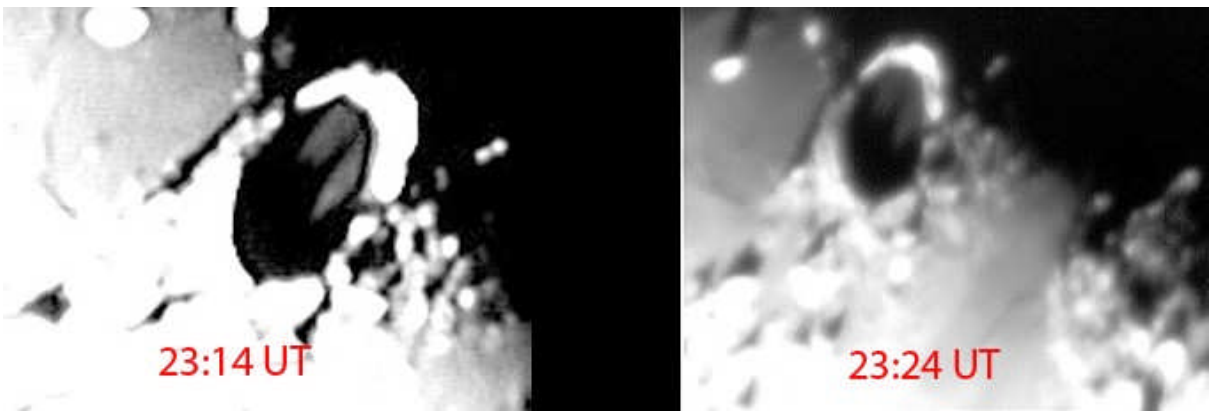

Fig. 6: Plato streaks as imaged by Bellido on May 16, 2005, at 23:14 UT

5. Observing Plato when illumination matches the #1027 TLP. Observations and digital images.

On 9 May 2003 at 18:25 UT Lena detected two streaks that matched Kelsey's description. The drawing, obtained using a 10 cm f/15 refractor, is shown in Fig. 4, and the appearance is similar to old observations reported by Fauth and Schröter (Figs. 1 and 2). The drawing corresponds to just 15 minutes after the repeat illumination for event #1027. The two streaks were elongated, extending gradually in a shaft of light to the western wall of Plato. These streaks appeared to fluctuate sometimes due to subtle oscillation of the seeing (III Antoniadi Scale) with a slight enhancement in red filter (W 25A) compared to blue filter (W 80A). Another observation carried out independently on the same night as Lena's drawing was made by Marie Cook, reporting the same two streaks (see Cook, 2003). She also had non-ideal atmospheric transparency to view the Moon through (compare Fig. 4a and 4b). The streaks were faintly visible in both red and yellow filters and hardly visible in blue filter. The two streaks were imaged by Bellido, Phillips and Shaw on 16 May 2005 at 23:14, 19 March 2005 at 02:17-02:58 UT, and 18 January 2005 at 23:59 UT, respectively (see Figs. 5 and 6). Fig. 7 shows another image made by Salimbeni during an observation carried out on 14 July 2005 at 19:46 UT. Furthermore, in a visual observation, the two streaks showed a slight enhancement in red light compared to blue light in agreement with Kelsey's report. We deduce that the enhancement in red filter is considered as "a natural blink" for the Plato crater. Mobberley (1986) examining the spurious colour in Plato described this effect as due to the oblique angle at which Plato is observed. This causes red to appear more prominent than blue on the inner north wall and blue to be more prominent than red on the top of the south wall (Marshall & Mobberley, 1986).

Several independent observations on different dates indicate strongly that this phenomenon is a normal effect where light from a rising Sun starts to stream over low points in the crater wall and reaches the mostly shadow filled floor forming elongated patches/streaks of light. Further confirmation was received from an observation by Cicognani (Fig. 8) carried out on 20 November 2004 at 18:00 UT. Cicognani reported also the presence of an elusive third streak as the Sun rose higher, showing how rapidly the appearance of the crater changes with increasing solar elevation. Thus two thin shafts of light are what one would expect from a normal topographic pattern illuminated by a steadily rising Sun.

6. Topographic measurement of the east rim

The extension of patch of light outward from a centre originating on the crater floor is exactly what one expects from a "valley" (here defined as Low Point) located on the eastern rim. The eastern edge of the patch of light is defined by the Moon's curvature. It is the point where the Sun's rays are tangent to the general surface – that is, the point where the rising Sun can first be seen. As the

Sun angle increases, the eastern edge of the patch will extend further over the Moon's curve, and the western edge will approach the foot of the crater wall (reaching it when the local sun angle equals the slope of the wall). As shown in the image taken by Acquarone on 28 December 2006 at 18:31 UT (Fig. 9a), three valleys may be detected in the east rim of Plato. The lowest (here named "Low Point 1") is located at longitude -6.74° W and latitude 52.30° N. It is probably the point where the Sun' rays, shining over this gap, produce the northern spot/streak of light. Two other gaps in the east wall are detectable in Fig. 9, located at coordinates of 6.89° W and 51.10° N (Low Point 2) and 6.67° W and 51.56° N (Low Point 3) respectively. Table 3 reports their elevations computed from Fig. 9b. The measurements were made using the LTVT software package of Mosher and Bondo (2006) as described in Section 4. A spot of sunlight is thus expected from Low Point 1 that descends from a height of about 1520 m above the crater floor, extending gradually. This streak will be followed very shortly afterwards by a spot of light from Low Point 2 with a computed elevation of about 1770 m and then from Low Point 3, with an elevation of about 2090 m, likely responsible for the elusive third streak. Based on this result we infer that during Kelsey's observation the sun angle at Low Point 1 was 2.38°. Furthermore, for comparison we computed, for our observations, the solar angle over Low Point 1 (Table 4). Note the different extension of the patches and how rapidly the appearance of the crater changes with increasing solar elevation (Figs. 4-8 and Table 4). Furthermore, our first observation (Fig. 3) was made when the sun angle at Low Point 1 was 2.39°.

7. Plato's floor topography : result and discussion

In this section we will examine if the appearance of the streaks may be due to a raised topography (Section 7.1) or to the effect of the lunar curvature (Section 7.2).

7.1 Measurements in sunset

The interior of the crater Plato displays a classic smooth floor and the Clementine LIDAR data suggest that the floor of Plato is flat. In order to identify if a slightly raised topography could account for the shape of two streaks reported under shallow illumination (e.g. Figs. 4a and 4b) we have computed the coordinate and the height of a peak on the western wall (located at longitude of 11.98° W and latitude of 52.04° N) from shadows of different lengths. The measurements were obtained using the shadow length tool in the LTVT software package of Mosher and Bondo (2006) after calibration of all the images taken near sunset and described in Table 5 (Fig. 10-13). We estimated the error by making several measures of the shadow casting points. On this basis the error bar is calculated to be 5% of the value (Fig. 14). The computed heights are plotted relative to distance along the crater floor without any significant variation of the profile. The height measurements are consistent which each other due to the fact that their error intervals overlap. Similar results were obtained using

different peaks on the western wall. Thus if there is any abnormal convexity to the floor of Plato it is too slight to detect by this method.

7.2 Measurement in sunrise

Mosher (private communication) illustrates a general approach for calculating the expected extent of the illuminated region behind a raised point on a curved lunar surface. The point could equally well be an isolated peak or a feature at the top of a crater rim. The three simple formulas given in Appendix A are all that is necessary to calculate the location and extent of the illuminated zone behind a peak on a curved surface. The data required are the radius of the curved surface, the height of the peak (or a low point above that surface) and the Sun angle (relative to the local horizontal) at the peak or low point. These are used to calculate the first and last points of sunlight on the surface behind the raised point. When the Sun angle is $\alpha = 0$, the sunlight streaming over the raised point will completely miss the surface: everything beyond the peak will be in shadow, and the two points on the lunar surface are undefined. The first touching of rays to the surface occurs when the sun angle reaches a critical angle α_0 such that the rays are just tangent to the curved surface. Under this condition the two points on the lunar surface are the same. Taking the typical curve of the lunar surface as R = 1738 m, the method reported in Appendix A (Eq. 4) indicates that rays from the Sun's center would first reach the surface (giving it ~50% illumination) when the sun angle at the low point 1 on the east rim of Plato (with an elevation H of 1.52 km as estimated in section 5) is:

$\alpha_0 = \text{ArcCos}[R/(R + H)] = 2.39°$

In radians this is $2.39\ (\pi / 180) = 0.0418$. Therefore the expected distance from the rim to the illuminated point on the crater floor is computed as follows:

$L_0 = 1738 \text{ km} (0.0418) = 72.6 \text{ km}$

Kelsey's observation was made on 18 April 1967 at 03:10 UT, when the Sun angle at east rim Low Point 1 is computed to be 2.38°, which is in excellent agreement with the prediction model based on Plato's floor following the normal curvature of the Moon. A spot of sunlight would have been expected on the crater about 72 km from the east rim. Further streaks will appear as spots of light from Low Point 2 and then Low Point 3. This result demonstrates strongly that the Kelsey's event (entry #1027 in the Cameron catalog), and further similar observations reported in Section 2, are not a TLP events but the normal appearance of this crater. Further conclusions may be drawn:

- An experienced observer might possibly be able to see the first rays from the Sun's upper limb, which touch the surface when the Sun's center is still 0.25° below the critical angle. This would advance the timing of the first light to the point when the Sun's center reaches an angle of 2.39–0.25=2.14°

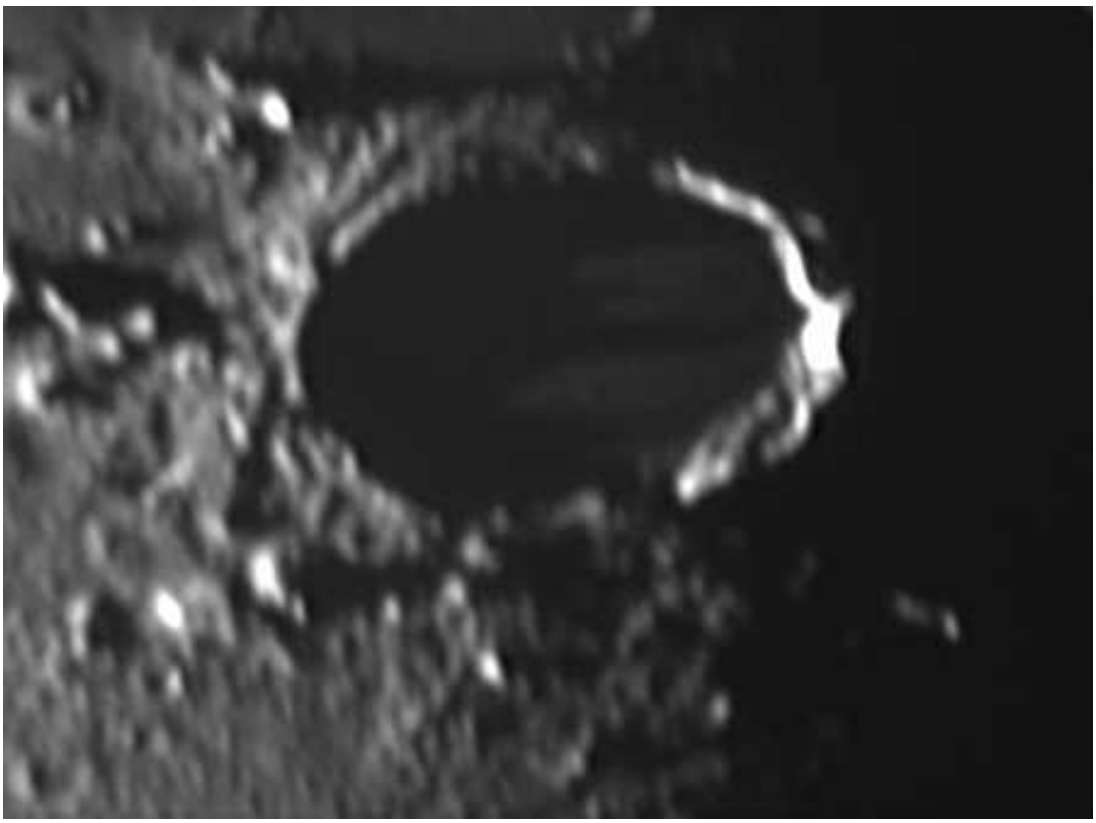

Fig. 7: Image taken by Salimbeni on 14 July 2005 at 19:46 UT.

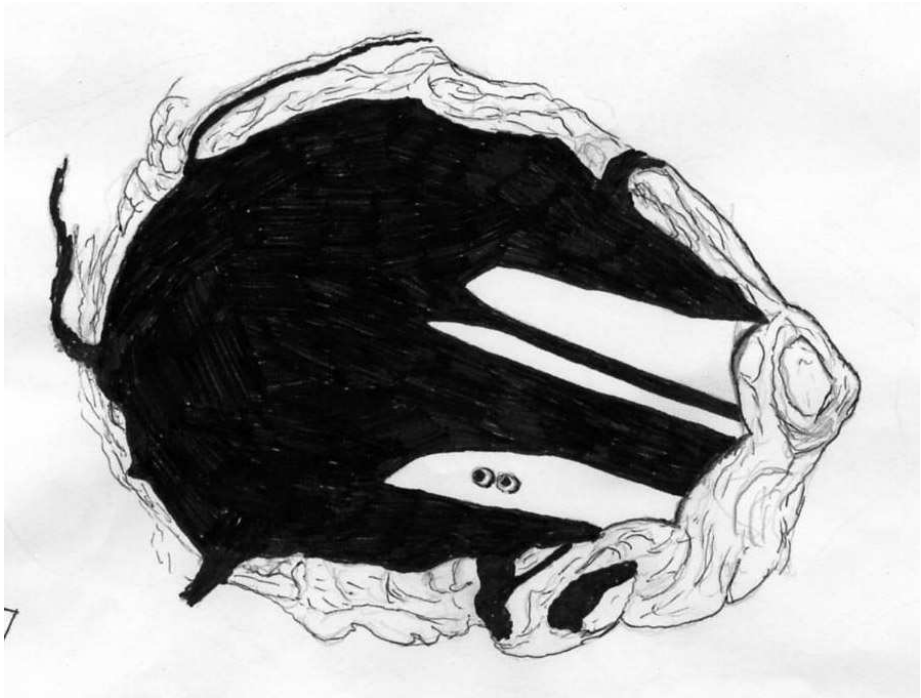

Fig. 8: Plato as drawn by Cicognani on 20 November 2004 at 18:00 UT.

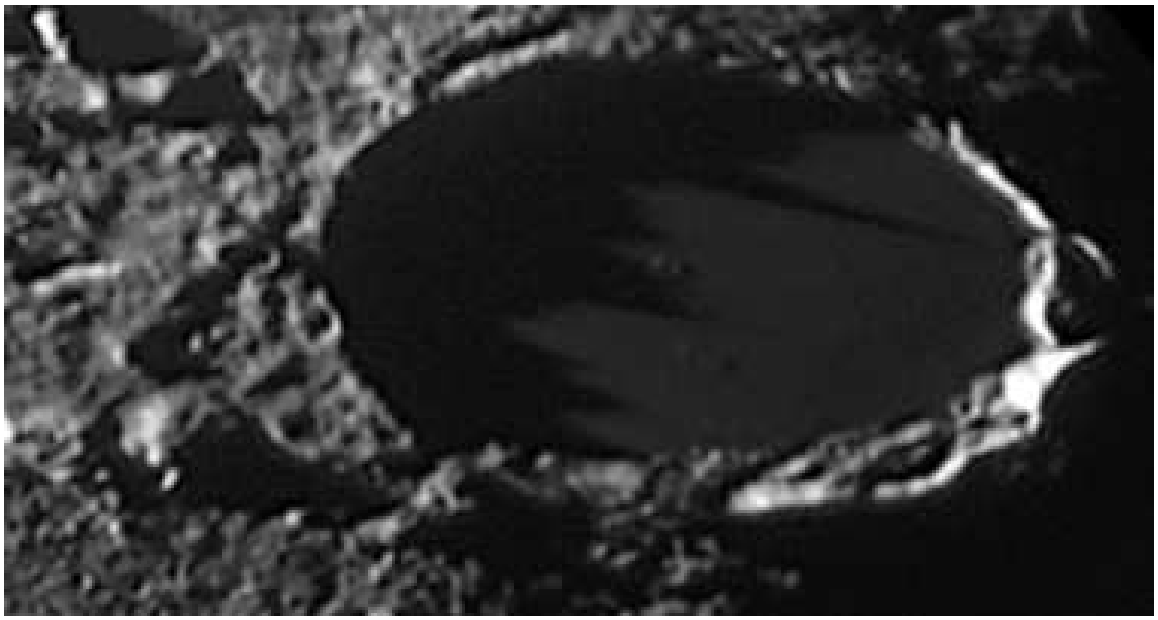

Fig. 9a: Image taken by Acquarone on 28 December 2006 at 18:31 UT.

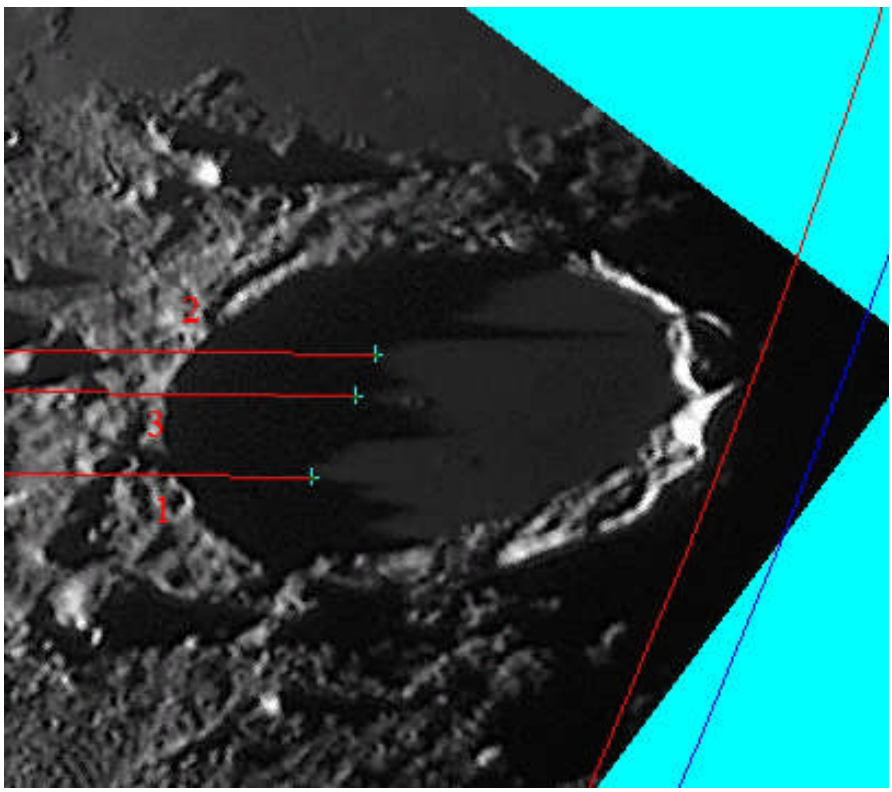

Fig. 9b: Coordinates of three low points in the east wall determined on Fig. 9a with the LTVT software by Mosher and Bondo (2006).

relative to the horizontal plane at Low Point 1. Under this assumption we may infer that the first light could be seen at 2.54–0.25=2.29° relative to Low Point 2 and 2.81–0.25=2.56° relative to Low Point 3.

- Table 7 reports the solar altitudes computed for our images and drawings along the critical angle α_0 such that the Sun's rays are just tangent to the surface. The resulting data are in excellent agreement with the predictive model also for the visibility of the third streak (see Figs. 4-8). We suspect that many other TLP reports involving events during local lunar sunrise are similarly normal appearances. Future observing schedules are being planned to investigate each of these on a case by case basis. It is hoped that by eliminating many of the less reliable reports in the catalogs, we will be left with a core set of observations upon which more reliable statistical analysis of the nature of TLP reports can be performed.

Acknowledgements: We wish to thank all the observers for their contribution to this paper during a GLR survey. We are grateful to the BAA for the mentioned data. We extend our thanks to T. Cook for some comments about combined observations described in the webpage http://www.cs.nott.ac.uk/~acc/Lunar/2003may.htm. A special thanks to Jim Mosher for the predictive model described in Appendix A and for his stimulating discussions.

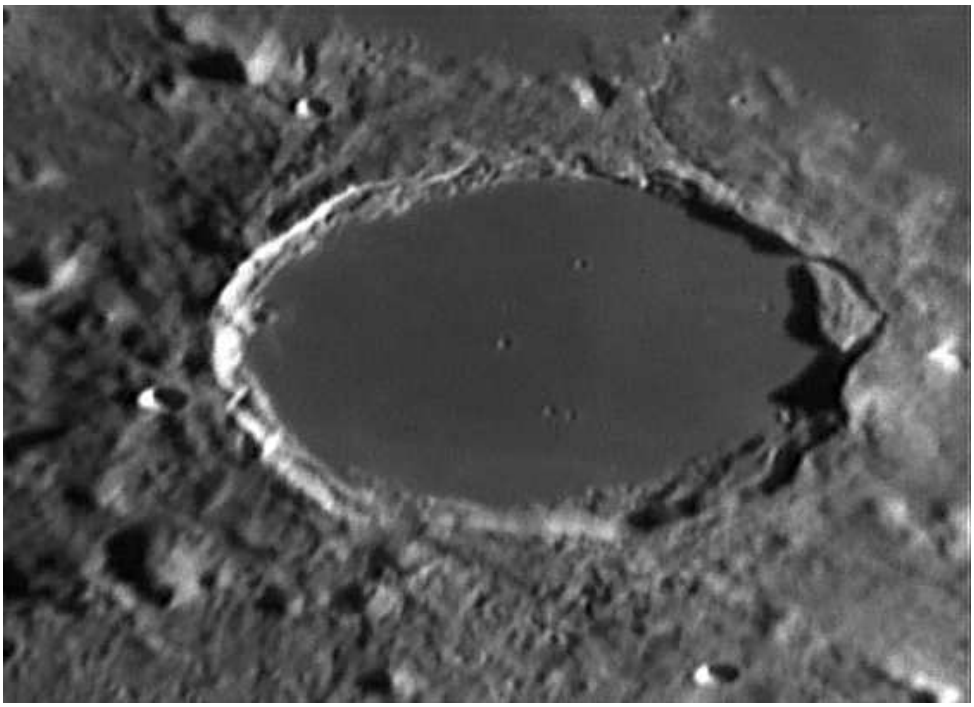

Fig.10: Image taken by Fattinnanzi on 2 January 2005 at 03:33 UT (sunset)

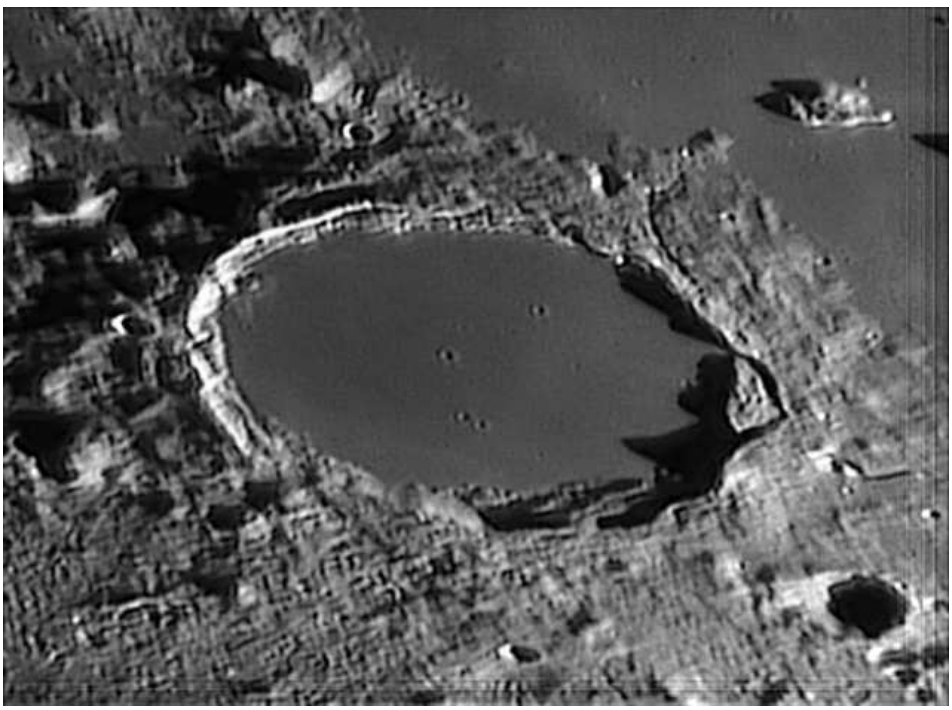

Fig. 11: Image taken by Fattinnanzi on 6 October 2004 at 04:44 UT (sunset)

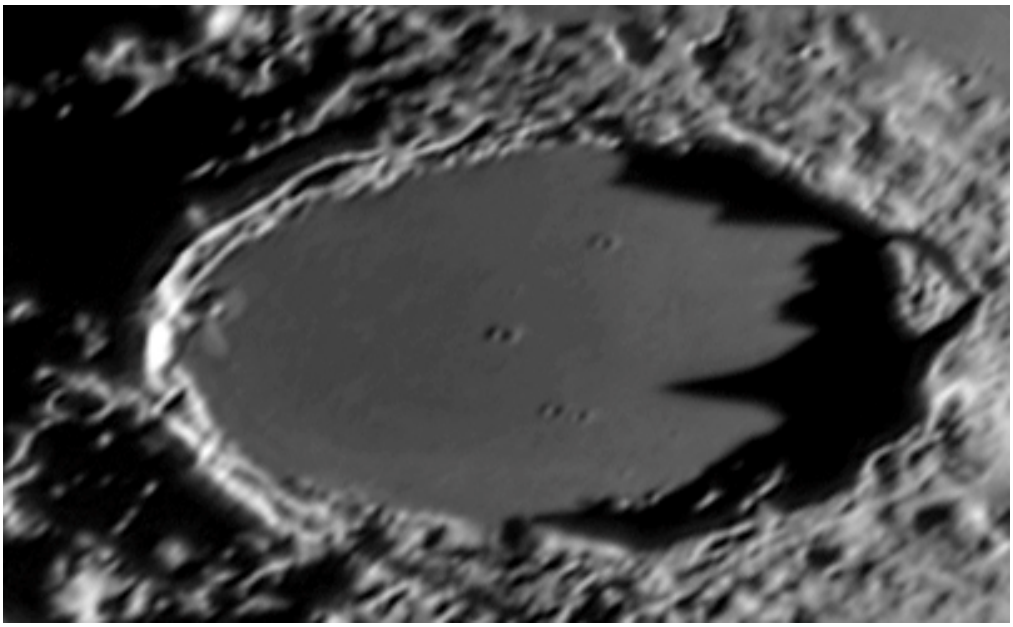

Fig 12: Image taken by Bianconi on 5 November 2004 at 03:21 UT (sunset)

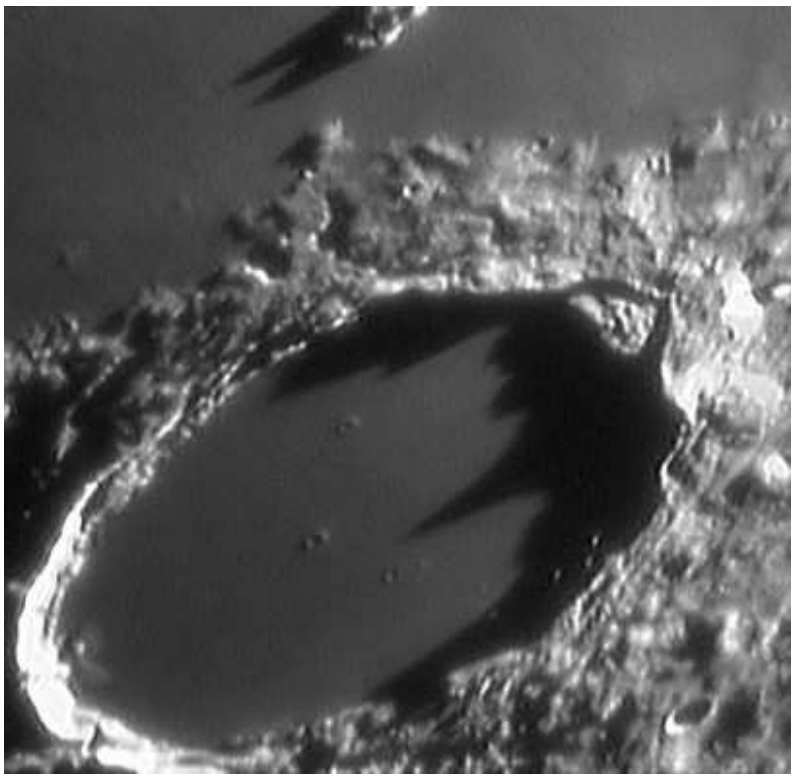

Fig 13: Image taken by Higgins on 18 October 2003 at 11:12 UT (sunset)

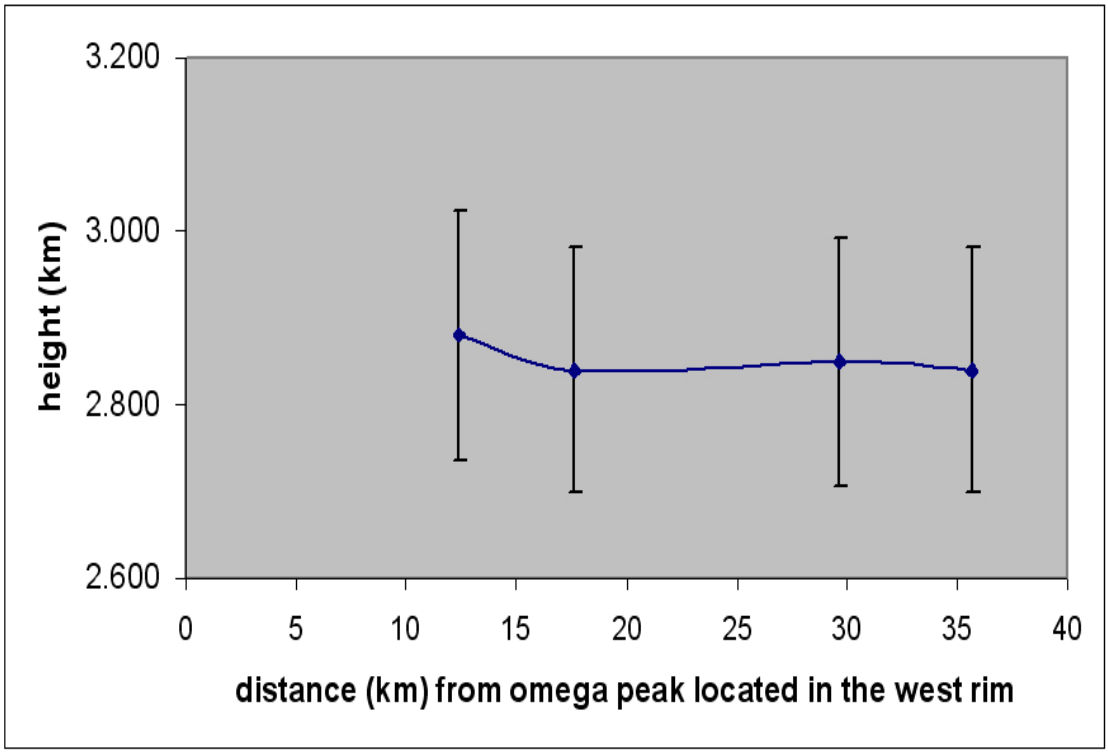

Fig. 14: The computed heights are plotted relative to distance along the crater floor without any significant variation of the profile. Data obtained based on the images shown in Figs. 10-13 in sunset.

References

[1] Cameron, W., Comparative analyses of observations of lunar transient phenomena, 1972, Icarus, 16, 339.

[2] Cameron, W., Lunar Transient Phenomena Catalog, 1978, NSSDC, NASA-TM-79399, 109 pages.

[3] Cameron, W., Lunar Transient Phenomena Catalog Extension, 2006, NSSDC/WDC-A-R&S,7803, 152 pages (http://www.cs.nott.ac.uk/~acc/Lunar/catalog.pdf).

[4] Cook, A., BAA 2003- http://www.cs.nott.ac.uk/~acc/Lunar/2003may.htm

[5] Crotts, A., Transient Lunar Phenomena: Regularity and Reality, 2007, arXiv:0706.3947v1, http://www.astro.columbia.edu/~arlin/TLP/paper0.pdf

[6] Crotts, A., Lunar Outgassing, Transient Phenomena and The Return to The Moon, I: Existing Data, 2007, arXiv:0706.3949v1 , http://www.astro.columbia.edu/~arlin/TLP/paper1.pdf

[7] Crotts, A., Hummels, C., Lunar Outgassing, Transient Phenomena and The Return to The Moon, II: Predictions for Interactions between Outgassing and Regolith, 2007, arXiv:0706.3952v1, http://www.astro.columbia.edu/~arlin/TLP/paper2.pdf

[8] Crotts, A., Lunar Outgassing, Transient Phenomena and The Return to The Moon, III: Observational and Experimental Techniques, 2007, arXiv:0706.3954v1, http://www.astro.columbia.edu/~arlin/TLP/paper3.pdf

[9] Jamieson, H. D., The Lunar Dome Survey – Fall, Strolling Astronomer, 1992 Progress Report, 1993, 37 (1), p 14-17.

[10] Lena, R., Cook, A., Emergence of low relief terrain from shadow: an explanation for some TLP, 2004, J. Brit. Ast. Assoc., 114, 136.

[11] Marshall, K.P., Mobberley, M. P., The lunar crater Plato, 1986, J. Brit. Ast. Assoc., 96, 156-165

[12] M'Gonigle, J. W., Schleicher, D., USGS I-701 map, Geologic Atlas of the Moon Plato quadrangle 1972.

[13] Middlehurst, B.M., Burley, J.M., Moore, P. , Welther, B.L., 1968, Chronological Catalog of Reported Lunar Events, NASA Tech. Rep. TR R-277 http://www.mufor.org/tlp/lunar.html.

[14] Middlehurst, B., A survey of lunar transient phenomena, 1977, Phys. Earth Planet. Inter., 14, 185.

[15] Mosher, J., Bondo, H., 2006. Lunar Terminator Visualization Tool (LTVT).

http://inet.uni2.dk/ d120588/henrik/jim ltvt.html

[16] Pike, R. J., Crater dimensions from Apollo data and supplemental sources, 1976, The Moon, 15, 463-477.

[17] Robinson, R., 2003, Lunar Sunrise/ Sunset Crater Rays,

http://www.lunar-ccultations.com/rlo/rays/ plato.htm

[18] Schröter, J., Selenotopographische Fragmente zur genauern Kenntniss der Mondfläche, 1971, vol. 1, Lilienthal: auf Kosten des Verfassers.

[19] Webb, T. W., Celestial Objects for Common Telescopes, 1962, Vol. 1, Dover Publications.

[20] Wood, C. A., Central Peak Heights and Crater Origins, 1973, Icarus, 20, 503.

Table 1: Observers who submitted observations which match the lighting conditions for the April 1967 Plato event #1027

Observer	Telescope	Diameter	f/N	Method	N° of
F. Bellido	Maksutov-Cassegrain	12 cm	f/12	Webcam	1
M. Cicognani	Cassegrain	41 cm	f/17	Visual	1
R. Lena	Refractor	10 cm	f/15	Visual/ Digicam	4
J. Phillips	Refractor	25 cm	f/9	CCD	2
Pg. Salimbeni	Schmidt Cassegrain	20 cm	f/10	Visual/ Webcam	2
B. Shaw	Newtonian	25 cm	f/9	CCD	2

Table 2: Observations which match the lighting conditions to within +/- 0.1° for the April 1967 Plato event #1027. The solar altitude was computed for the centre of Plato (longitude -9.3° latitude +51.6°)

Date	**UT**	**α (°)**	**Col.(°)**	**Az.(°)**	**Sun's selenog. Lat. (°)**	**Librations** **Lat.**	**Long.** **(°)**
18 April 1967	03:10	0.8°	11.0°	91.5°	-0.30°	-7.6°	-6.7°
9 May 2003	18:10	0.8°	11.0 °	91.6°	-0.34°	-7.7°	-6.7°
20 November 2004	15:50	0.9°	11.7°	92.3°	-0.72°	+6.3°	+4.8°
18 January 2005	22:45	0.9°	12.6°	93.2°	-1.55°	+6.4°	-2.3°
19 March 2005	00:30	0.8°	11.5°	91.6°	-0.69°	+1.8°	-6.6°
14 July 2005	17:55	0.9°	8.9°	88.67°	+1.54	-7.5°	-0.7°

Table 3: Coordinates of three low points in the east wall and their elevation computed on fig. 9b

Low Point	Longitude (°)	Latitude (°)	Height [km]
1	-6.74°	52.30°	1.52
2	-6.89°	51.10°	1.72
3	-6.67°	51.56°	2.09

Table 4: Data about the observations concerning the lighting conditions for the April 1967 Plato event #1027. The solar altitude is computed for the low point 1, the lowest valley in the east wall of Plato (located at longitude 6.74° W and latitude 52.30° N).

Date	**UT**	**α (o)**	**Col.(o)**	**Az.(°)**
18 April 1967 (Kelsey #1027)	03:10	2.38°	11.00°	93.57°
9 May 2003 (Fig. 4a)	18:10	2.39°	11.07 °	93.64°
19 March 2005 (Fig.5a)	02:17	2.93°	12.43°	94.95°
16 May 2005 (Fig. 6)	23:14	3.04°	10.58°	92.51°
14 July 2005 (Fig.7)	19:46	3.07°	9.77°	91.46°
20 November 2004 (Fig.8)	18:00	3.15°	12.84°	95.27°

Table 5: Observers who submitted observations which were used for a study about variations in the floor topography.

Observer	Telescope	Diame-ter	f/N	Method	Fig-ure	Date/ Time UT	Col (°)
A. Bianconi	Schimdt Cassegrain	41 cm	f/17	Web-cam	12	5 November 2004, 03:21	182.56°
C. Fattinnanzi	Newtonian	25 cm	f/5	Web-cam	10 11	2 January 2005, 03:33 6 October 2004, 04:44	168.16° 177.79°
W. Higgins	Newtonian	36 cm	f/4	Web-cam	13	18 October 2003, 11:12	185.52°

Table 6: Prediction of the critical angle α_0 such that the Sun's rays are tangent to the surface for the three low points located in the east wall of Plato.

Low Point	Longitude (°)	Latitude (°)	Critical angle α_0
1	-6.74°	52.30°	2.39°
2	-6.89°	51.10°	2.54°
3	-6.67°	51.56°	2.81°

Table 7: Data about the observations concerning the lighting conditions for the April 1967 Plato event #1027. The solar altitude is computed for the low points 1-3 along the Critical angle α_0

Date	**UT**	**Low Point 1 α** **Critical angle α_0=2.39°**	**Low Point 2 α** **Critical angle α_0=2.54°**	**Low Point 3 α** **Critical angle α_0=2.81°**	**Remarks**
9 May 2003 (Fig. 4a)	18:10	2.39°	2.36°	2.47°	Two streaks
19 March 2005 (Fig.5a)	02:17	2.93°	2.95°	3.03°	Three streaks
16 May 2005 (Fig. 6)	23:14	3.04°	2.98°	3.12°	Three streaks
14 July 2005 (Fig.7)	19:46	3.07°	3.01°	3.14°	Three streaks
20 November 2004 (Fig.8)	18:00	3.15°	3.17°	3.26°	Three streaks

APPENDIX A

Calculation of Illuminated Region on a Curved Moon

Figures A-C illustrate a general approach for calculating the expected extent of the illuminated region behind a raised point on a curved lunar surface. The point could equally well be an isolated peak or a feature at the top of a crater rim.

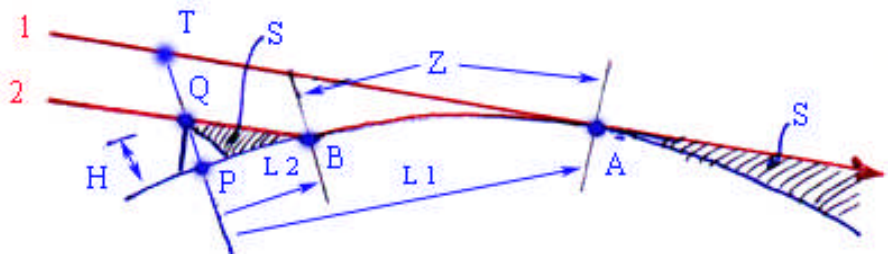

Figure A

C = center of Moon

R = radius from C to average lunar surface

Q = raised point on surface

P = projection of Q onto lunar surface following a radial line

H = height of peak = length of PQ

"1" = ray of light from Sun's center grazing Moon's surface at point A

"2" = ray of light grazing peak Q and striking surface at point B

L1 = distance (arc length) on Moon's surface from P to A

L2 = distance (arc length) on Moon's surface from P to B

S = areas in shadow (the region between P and B, and the region beyond A)

T = point where ray "1" crosses the radial line through Q

Z = zone on surface illuminated by sunlight (the region between B and A)

Moreover (see fig. B and C)

α = angle of Sun above horizontal at Q

β = angle from P to B as seen from Moon's center (i.e., the angle PCB)

γ = angle from Q to C as seen from B (i.e., the angle QBC)

Qualifications:

1) The diagrams are drawn in the plane containing P, C and the sub-solar point; and the formulas apply strictly only to the calculation of angles and distances in that plane.

2) The light rays represent those from the Sun's center. These are strictly parallel and in a continuously changing direction determined by astronomical calculation. Rays from the Sun's center above "1" miss the lunar surface; while rays below "2" are blocked by the peak. In reality, the Sun has an angular diameter of 0.5 degrees as seen from the Moon, so there are additional sets of rays at angles spread by as much as +/- 0.25 degrees with respect to the ones drawn.

Method of Calculation

1. To determine the location and width of the zone of illumination, we need only to calculate the two lengths L_1 and L_2.

2. Figure B shows the triangle used to calculate L_1.

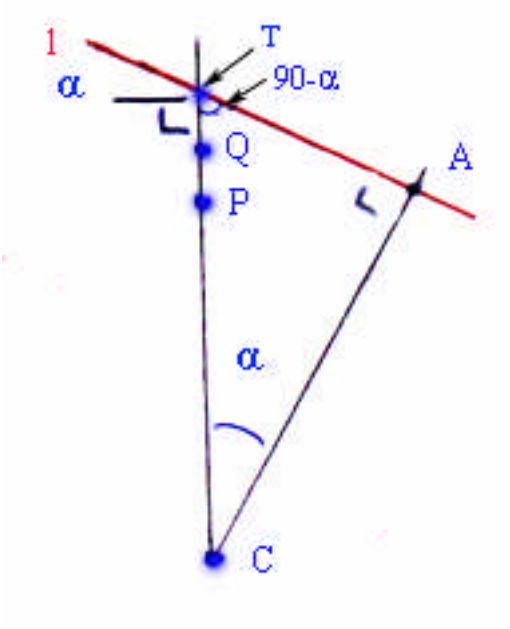

Figure B

3. The side CA is equal to the Moon's radius, R.

4. Because ray "1" is tangent to the curve of the lunar surface, the angle CAT = 90 degrees, as indicated.

5. The definition of the sun angle, allows angle α to be drawn above P, as shown. The angle α is measured relative to the local horizontal at P (or Q or T), represented by the short line perpendicular to the radial direction. The other two angles above P must therefore be 90° and (90° – α). From this, and the known angle at A, it follows that the angle PCA = α.

6. The arc length from P to A is totally determined by the angle PCA and the radius of the lunar sphere:

$$\mathbf{L1 = R * \alpha}$$

(where α is measured in radians) [Eq. 1]

7. Figure C shows the triangle used to calculate L_2.

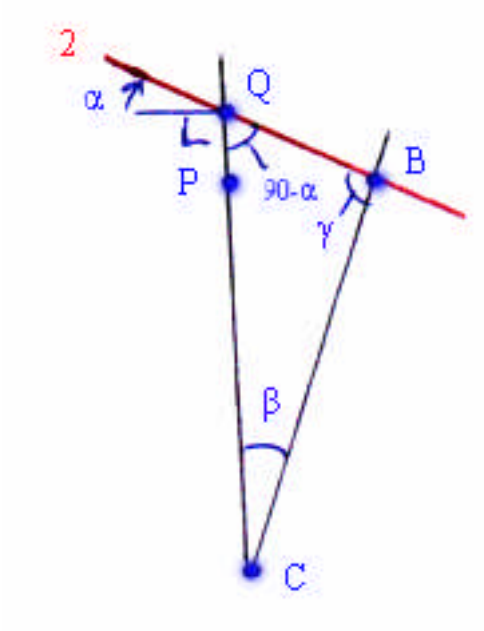

Figure C

8. As was done in Figure B, the sun angle, α, can be drawn at the top of the triangle and it follows that the inside angle of the triangle at this point (Q) is again (90 – α). However, this time the triangle contains two unknown angles: β (at C) and γ (at B).

9. To "solve" the triangle, we need to consider the known lengths of two sides. Since B is a point of the Moon's surface, the side CB has, by definition, a length R; while the side CQ has a length = R + H.

10. The angle CBQ = 180 – (90 – α) – α = 90 + α – β .

11. The so-called "law of sines" for plane triangles tells us that the ratio of the sine of the angle at B to the length of CQ is the same as the ratio of the sine of the angle at Q to the length of CB. From this it follows that:

$$\cos(\alpha) / R = \cos(\alpha - \beta) / (R + H)$$ [Eq. 2a]

which is equivalent to:

$$\beta = \alpha - \arccos[(1 + H/R) * \cos(\alpha)]$$ [Eq. 2]

12. The arc length from P to B is totally determined by the angle PCB and the radius of the lunar sphere:

$$L_2 = R * \beta$$

(where β is measured in radians) [Eq. 3]

Applications

1) time and location of first light

(sunrise event)

In connection with Plato, the main thing we are interested in is when and where sunlight streaming over a low point on the rim will first touch the curved surface.

When the sun angle is α = 0 (or less), the sunlight streaming over a raised point will completely miss the curved surface, so everything beyond that point will be in shadow. Under these circumstances, the points A and B (as drawn in Fig. A-C above) are undefined. The first touching of rays to the surface occurs when the sun angle reaches a critical angle α0 such that the rays are just tangent to the surface. Under this condition the points

A and B are the same, and $L_1 = L_2 = L_0$. Inspecting Equation 2, the condition for the equality of L_1 and L_2 implies that:

$(1 + H/R)*\text{Cos}(\alpha_0) = 1$ [Eq. 4a]

or

$\alpha_0 = \text{ArcCos}(R/(R + H))$ [Eq. 4]

This can be derived in other ways, but the result for this critical sun angle will always be the same, and tells us that the position where the spot of light will first be observed is defined by:

$L_0 = R * \alpha_0$ (where α_0 is in radians) [Eq. 5]

Note that the preceding calculation assumes rays from the Sun's center (the conventional definition of sun angle). This corresponds to a time when the illumination is roughly at the midpoint between total darkness and full sunlight. But the rays from the Sun's upper limb will obviously begin to touch the lunar surface before those from the center. If one was standing at the point of first light, one would begin to see the sun's upper limb peeking above the point Q when the Sun's center is approximately 0.25 degrees below that point. So if one wishes to determine the moment when the very first faint first illumination will be visible, the critical angle should be decreased by 0.25 degrees to allow for this.

2) Behaviour after first light

Examination of the Equations 1-3 shows that as the Sun rises ($\alpha > \alpha_0$), the distance L_2 (to point A) increases steadily ($L_2 > L_0$). This is simply the normal angular advance of the lunar terminator. The distance L_1 (to point B) decreases gradually ($L_1 < L_0$) approaching a value of $L_2 = 0$ if it were possible for the Sun to be directly over P (if not, there will always be some shadow from P to B). As the result of these changes, the initially illuminated point at distance L_0 from P remains illuminated, but the width of the illuminated zone, Z, around it steadily increases. At any moment, the length of the illuminated arc is $L_2 - L_1$.

On the Moon we are interested in the pattern of light produced not just by a single point, but by a whole array of points along a ridge or crater rim. Each point can be thought of as producing its own streak of light of a length and at a position as described above.

The observed pattern will be the superposition of all these independent streaks.

3) Behaviour at sunset

The calculation, and therefore the behaviour, of the patch of light beyond a lunar peak at sunset is precisely the same as at sunrise, except in reverse sequence.

The initially long streak will effectively dry up into a tiny puddle at the same distance L_0 calculated above.

And just as the initial rays from the Sun's upper limb will be seen about 0.25 degrees before the Sun reaches the critical angle at sunrise, a sharp-eyed observer may likewise see the final rays for about 0.25 degrees after the Sun has passed below the critical angle at sunset.

A New Approach to Drawing Lunar Features
White chalk on black paper lunar sketching techniques

By Richard H. Handy
Member of the San Diego Astronomical Society

Co-author with Sol Robbins, Erika Rix, David Moody and Jeremy Perez of "Astronomical Sketching: A Step-by-Step Introduction" Springer Science + Business Media, LLC, (c) 2007

Webmaster, Astronomy Sketch of the Day (www.asod.info)

Abstract

From Galileo to Harold Hill and the contemporary sketches of Longshaw, Ebdon and Grego, lunar sketching has long been a vital and essential tool for understanding of lunar topography. To the wide variety of media utilized to draw the Moon's features, the Author wishes to add his preferred medium, white chalk on black paper sketching techniques.

Introduction

From the first drawings of the Moon produced by Galileo in his "Sidereus Nuncius" to the works of such scholarly observers as Schroter, Lohrmann, Beer, Madler, Schmidt, Neison, Elger, Birt, Krieger and Fauth, to the recent drawings of Harold Hill and Alika Herring, and the contemporary drawings of Nigel Longshaw, Colin Ebdon and Peter Grego, lunar sketching has been and still remains a vital and essential tool for understanding and describing lunar topography.

Although the general aim of lunar sketching is the same for everyone, which is accurate rendition of lunar features, the media utilized is surprising for its variety. These include but are not limited to graphite pencil, pen and ink stippling, ink wash, charcoal, and chalk or pastel sketching as well as computer graphic techniques.

Each medium has its own unique set of advantages that can be used by the observer to accurately depict the Moon's surface. Lunar sketching presents the observer with several interesting and challenging conditions. Apart from the constantly varying atmospheric turbulence and the collimation or the optical qualities of the telescope, and more specific to the Moon itself, they include the rapid advance of the terminator, the broad range of albedo values and the complexities of terrain textures. When sketching a feature on or near the terminator, shadow lengths change quite rapidly, and in as little as 30 minutes the details of a scene can change quite dramatically.

The Moon's range of surface brightness is remarkable, from an intense white, through a wide variation in gray, to a deep black. Lunar topography can be as smooth as a mare or as rugged and chaotic as a basin ring mountain range. The white on black sketching technique provides ways to rapidly create accurate drawings and the ability to render any observed gray tone or depict any lunar terrain.

In the Fall of 1999 I began working at the eyepiece of my 20" f/4.5 Dobsonian

telescope, working using a range of magnification between 65X and 475X to produce lunar sketches using white and black Conte' Crayons (TM) on black textured Strathmore (TM) paper. Although my first attempts were rather crude, I soon found myself very excited about the medium because as I learned to blend and apply the Conte', I discovered some valuable solutions to the difficulties associated with lunar sketching. Due to the speed of application and sketch development, I felt compelled to experiment with large 19" x 25" sheets of this thick (0.013") black, canvas textured paper which were taped to a drawing board. This in turn provided a unique opportunity to produce drawings that could be reasonably detailed yet encompass large regions of the lunar surface. Conversely, with an appropriately high magnification, I could record the details of a relatively small feature with a fair degree of precision. Currently I use a 12" f/10 SCT on a german equatorial mount with and without a binoviewer at magnifications between about 80X and 600X.

Materials and methods

The following is a presentation of the medium and a description of the way I approach the creation of a white chalk on black paper sketch. Hopefully it will serve as a useful guide for other observers attracted to this medium. First of all, the tools required with this medium are not much different at all from those used in pencil techniques. Along with the Conte' white and black Crayons, I use several types of erasers from art gum, Sanford Magic Rub to Pink Pearl, a sanding pad and pencil sharpeners, and a brush for removing eraser debris (see Figure 1).

In addition to these tools, I use paper blending stumps as well as natural and synthetic sponges or foam of various sizes as shown in Figure 2. Note that white blenders are separated from black blenders so that when I sketch I don't pollute delicate tonal areas.

In preparation for the sketch, the black paper is taped to a drawing board (see Figure 3). This can be a piece of 1/8" to 1/2" thick pressboard, plastic sheet or a smooth wood panel large enough to allow an entire 19 "x 25" sheet be held down to the surface using 2" wide masking tape. Black paper of a smoother texture can also be purchased in 9" x 12" pads, so a suitable drawing board can be as simple as a clipboard. When using the larger 19" x 25" paper, overlapping the paper at the edges with 0.5" of masking tape will result in a 18" x 24" final sketch size after the tape is pulled off the paper and board. Although I often hold the sketch board in hand, a suitable easel is also something I frequently use. My easel is a step ladder with a couple of 1/2" wooden dowels inserted into holes drilled into the top tray. This prevents the drawing board from slipping off the top ladder tray as the sketch progresses. Before beginning the sketch, I prefer to spend about a half hour to an hour carefully observing the selected target and it's environs. My attention is drawn to the brightest features, frequently crater rims and mountains, and the darkest areas which are generally their shadows or the area near the terminator on the unlit side.

I like to characterize the terrain as either composed primarily of mare, highland or plains units. Finally, during this period, I identify the area of the Moon I want to include in my sketch. First I must decide

Figure 1: This is a picture of my drawing ray with the type of sketching equipment I always have on hand.

Figure 2: The various paper blending stumps and natural or synthetic sponges or foam used to blend the Conte' Crayon.

how to orient the sketch, for example, with the length running perpendicular, parallel, or at an arbitrary angle to the terminator. The next thing I do before I start is to find a place that is exciting visually for its contrasts between light and dark.

The terminator is therefore my favorite "place" along which to locate such dramatically lit lunar features. Once I've decided to sketch a particular crater or feature, I will simply draw the most prominent crater or feature at a size that will allow me to include my composition in the frame of the page. So it comes down to this; the size and positions of all other craters and features take their scale from the size and position of the most prominent crater or feature. I draw the main crater the size I want to fit my page and all other features are constantly compared for size and position to this. Initially this starts as simple line work (see Figure 4).

Next, I use the side of the white Conte' stick and rub it against the page to start creating the mid tones and simultaneously define the shadow boundries. I call this "freezing the shadows" because it's at this point I start fixing the angle of the light as I observe it at the moment (see Figure 5).

Here you see that I'm continuing to apply the white Conte' to delineate the mid tones across the mare environs these craters sit amidst. Note that I've defined the shadows for smaller features (see Figure 6).

So what do we do with those blenders? Here you see the result, on the left hand side of the sketch, of using a synthetic sponge moved rapidly in a roughly randomized pattern over the built up Conte' Crayon. Conte' Crayons blend incredibly smoothly, and the way this toothy textured black paper can load up with chalk is simply amazing.

This characteristic will become more apparent as the sketch progresses (see Fig. 7).

More Blending and building up white Conte', at times I'm using paper blending stumps (particularly in tight places such as directly around crater rims or small features) and at times I switch back to sponges or pieces felt cloth for the larger areas.

Here you see the continuation of the buildup and blending process (see Figure 8).

Yet more blending, you can see how subtle the gradations in tones are and how easily attainable they are with this medium (see Figure 9).

Finally as shown in Figure 10, I darken the shadows with a black (Noir) B Conte' stick and finish the shading details, such as the fine structure in the shapes of the jagged shadows that the craters project across the lunar surface.

Yet more black Conte' is applied to define the shadows, all the while continuing to build up white Conte' by rubbing vigorously and in a random pattern, smoothly redistributing the chalk in order to reach the appropriate tone value observed. This is the final result, "Encke and environs".

The only other procedure left is to remove the masking tape holding the sketch to the board and spray the entire sketch with a fixative so that it will not smudge when placed in the archive box.

Additionally, acid free tracing paper or newsprint is laid between each drawing.

Figure 3: A picture of my improvised easel made of a step ladder and the black paper taped to the drawing board. Note the 1/2" wooden dowels inserted into the top plastic tray to hold the drawing board in place.

Figure 4: To begin the sketch I draw the outlines of the most prominent feature, the large crater in the upper right. All of the rest of the features are then compared to this crater for relative size and position on the paper.

Figure 5: Using the side of the square sticks of white Conte' Crayon, the mid tones are laid down in such a fashion as to outline the extent and shapes of the shadowed features.

Figure 6: Continuing to add small details such as the shadows of the hills and small craters.

Figure 7: The use of sponge blenders to create uniform gray tones.

Figure 8: I use paper blending stumps particularly in tight places such as around crater rims and small features.

Figure 9: As the blending continues very subtle tonal differences can be developed.

Figure 10: The sketch is finished after touching up the shadows and blending the white Conte' to match the observed tones.

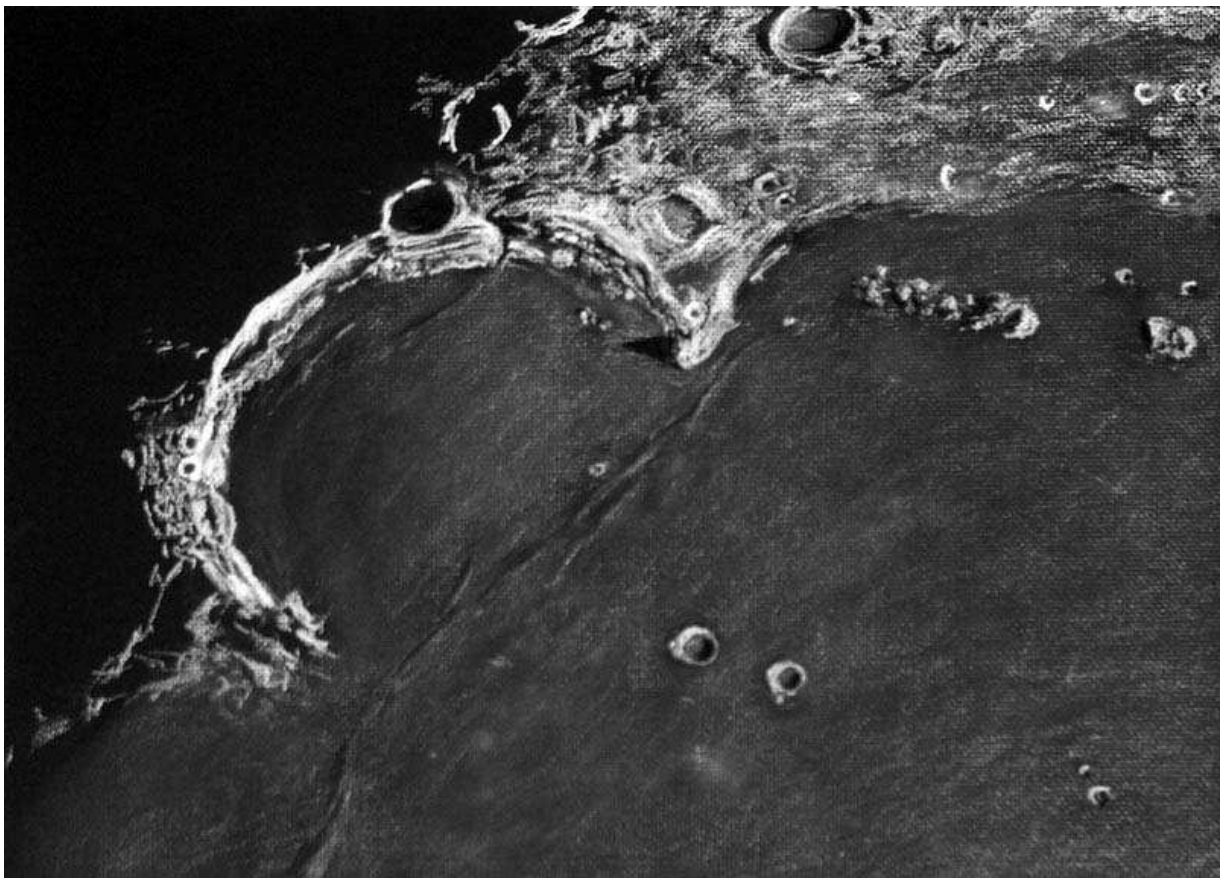

Figure 11: Large areas composed of widely varied terrain can be rendered using the white chalk on black paper medium as in this sketch of Sinus Iridum. Time: 4:47 UT till 6:10 UT Date: July 25, 2007 Seeing: Antoniadi III -II Weather: clear and calm Lunation: 10.7 days Colongitude: 35.8 deg. Illumination: 76.8% Lib. in Lat.: +07 deg. 31 min. Lib. in Long.: -03 deg. 28 min. Phase: 57.6 deg. Telescope: 12" Meade SCT f/10 Binoviewer: W.O. Bino-P with 1.6X nosepiece 45 deg. W.O. erect image diagonal Eyepieces: 20mm W.O. Plossls Magnification: 244X

Figure 12: Relatively small regions, such as this drawing of Bullialdus and environs, are easily attainable using an appropriately high power. Start- 4:30 UT End- 6:00 UT Date: 6-25-07 Lunation: 10.05 days Phase: 61.1 deg Illumination: 74.2% Lib. in Lat.= +5 deg 56 min Lib. in Long.= -00 deg 10 min Seeing: Antoniadi II to III Weather: clear Telescope: 12" SCT f/10 Bino viewer: W.O. Bino-P with 1.6X nosepiece Eyepieces: 12.4 mm Meade Super Plossls Magnification: 393X

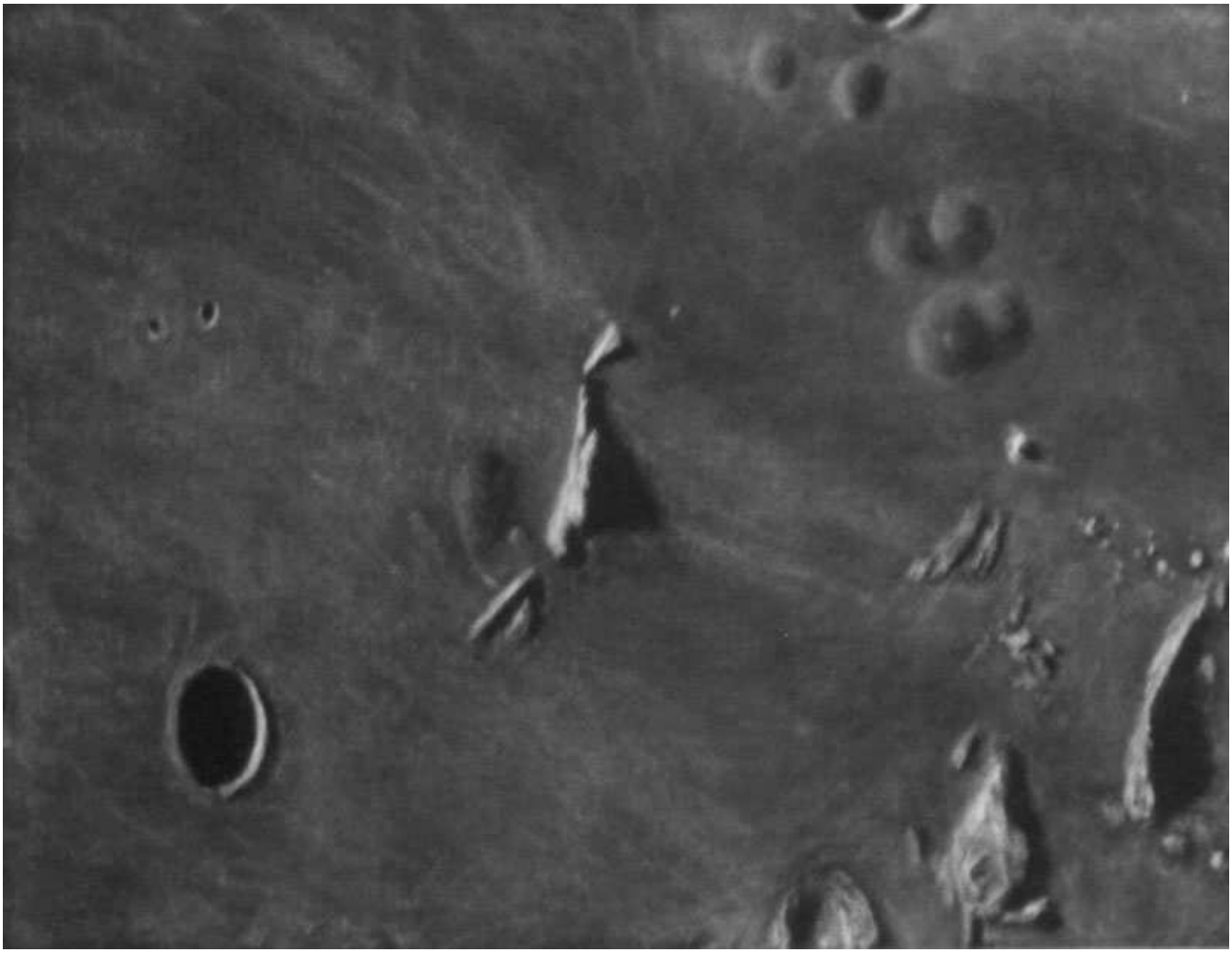

Figure 13: This sketch of the domes near Hortensius displays the variety of subtle detail such as the rays from Copernicus crossing the area and the soft shading of the domes. Date: 9-27-05 Lunation: 23.75 days Start time: 12:35 UT End time: 13:47 UT Seeing: Antoniadi III, IV Weather: Clear Scope: 12" Meade SCT Diagonal: 45 Degree Eye-piece: 20mm Plossl Barlow: 2X Magnification: 305X

Figure 14: Near the terminator, the dramatic difference between darkness and light paint intense views of the lunar surface which are often difficult to render. This sketch shows the usefulness of the white chalk on black paper medium in capturing such a transient scene. This is a drawing of Mare Humorum and the hallmark crater Gassendi as they sit straddling the terminator. Date: 9-4-06 Start time 4:20 UT Ending time: 5:56 UT Seeing: Antoniadi III with moments of II every 3-5 min, Weather: clear to partly cloudy Lunation: 11.38 days Colongitude: 46 deg Phase: 49.9 deg Illumination: 82.2 % Lib. in Lat. : +6 deg 28 min Lib. in Long.: - 6 deg 53 min Telescope: 12" Meade SCT F10 Binoviewer: W.O. Bino-P with 1.6X Nosepiece Eyepieces: W.O. 20mm W.O. Plossls Magnification: 244X

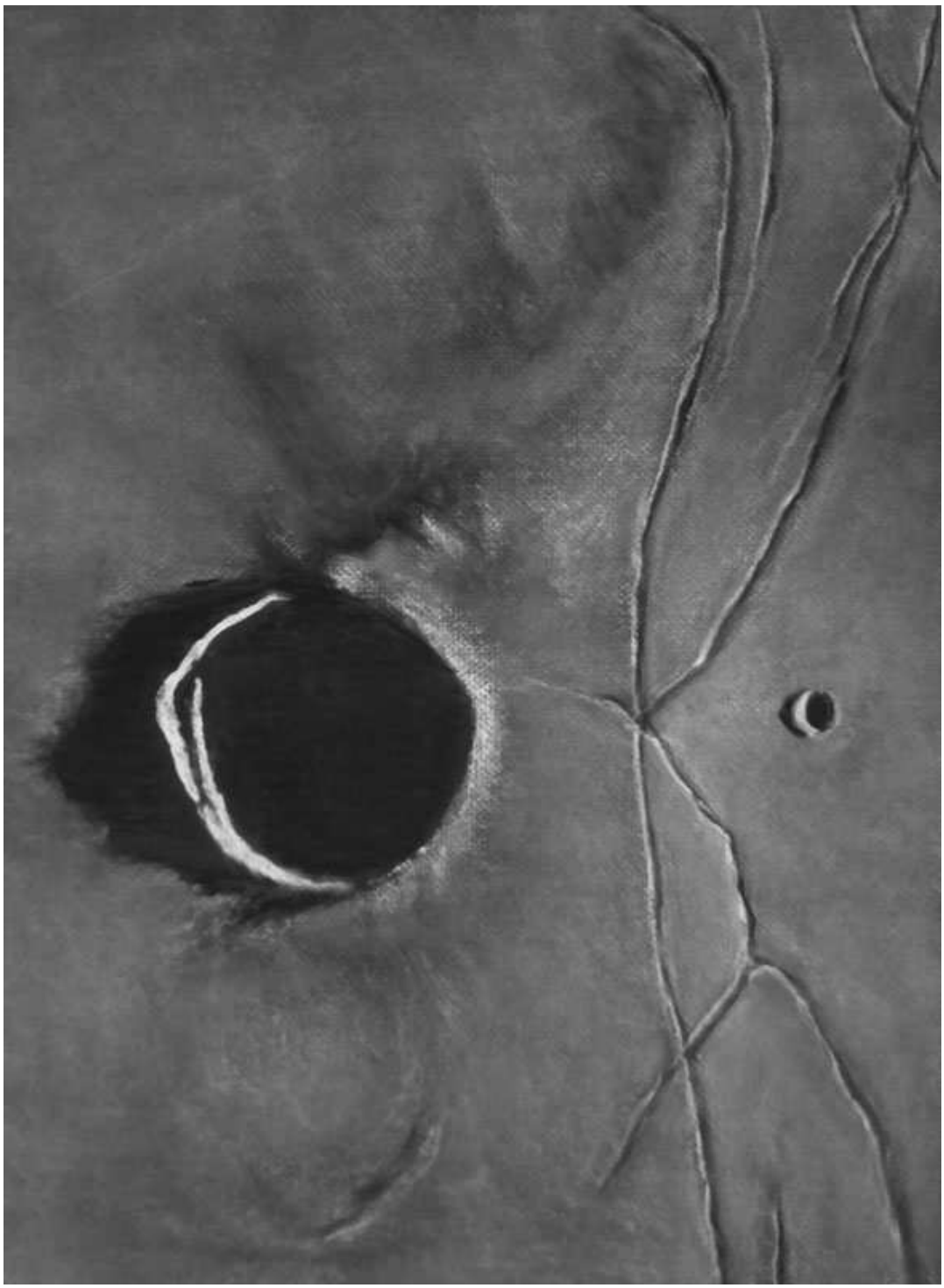

Figure 15: Yet another example of the delicate details such as the Triesnecker Rimae that can be captured using this white on black technique. Date: 1-26-07 Started- 4:38 UT End- 5:55 UT Lunation: 7.03 days Phase: 86.8 deg Illumination: 52.8% Colongitude: 359.7 deg Lib in Lat.: -4 deg 33 min Lib in Long.: +03 deg 35 min Seeing: Antoniadi III to IV Weather: Clear Telescope: 12" Meade SCT f/10 . Binoviewer: W.O. Bino-P with 1.6X Nosepiece. Eyepieces: W.O. WA 20mm Plossls Barlow: 2X Televue Powermate Magnification: 488X

Results and perspective

I have included Figures 11 through 15 as examples of finished sketches utilizing this white chalk on black paper technique. They illustrate the wide range of terrains, features and scales possible to render with this medium. This medium opens an exciting new frontier for anyone interested in its application to lunar sketching. Contemporary lunar sketchers whose superb work in this medium continues to inspire me include UK artists Sally Russell and Deirdre Kelleghan and American artists Frank McCabe, Erika Rix, and Jeremy Perez.

References

[1] Nigel Longshaw, "The Small Collection of Important Selenographical Works Held by the Manchester Astronomical Society". http://www.mikeoates.org/mas/cn/lunabooks/home.htm

[2] Harold Hill, "A Portfolio of Lunar Drawings", Cambridge University Press, © 1991.

[3] Peter T. Wlasuk, "Observing the Moon", Springer-Verlag London Ltd, © 2000. See Nigel Longshaw's drawings; pages 40, 51, 64, 91, 97, 101. See Colin Ebdon's drawings; pages 45, 47, 48, 62, 76, 80, 84, 98.

[4] Nigel Longshaw, Manchester Astronomical Society Personal Page http://www.manastro.co.uk/members/contrib/nlongshaw/index.htm

[5] Peter Grego, "The Moon and How to Observe It" Springer © 2005.

ANOTHER MOON DRAWING TECHNIQUE

By Maria Teresa Bregante
Geologic Lunar Research (GLR) group

Abstract
Harold Hill's lunar portfolio is a unique collection of drawings. These lunar drawings involve some difficulties like weak light and poor seeing that considerably affects the observation. In this article, I describe a technique for lunar drawings of the moon.

Certainly you have looked at the Moon and have been amazed by the sheer wealth of detail visible. If you have a small telescope, you can see many thousands of craters with their bright ray systems. Mountains, hills, domes, rilles, clefts, faults, valleys, dorsa (wrinkle ridges) can be seen. Lunar observation is undoubtedly the most visually rewarding branch of astronomy.

Most lunar observers regard the telescope eyepiece as if it were the porthole of their very own Apollo command module. The privilege of just seeing is satisfying enough. Four hundred years ago, when Galileo made his first telescopic observations of the Moon, he naturally had to make drawings to record what he had seen. For another three centuries, drawing remained the only way of recording what was seen at the eyepiece, until the advent of astronomical photography later in the 19th century.

Nowadays, the CCD technology is becoming ever more commonplace. Instantaneous and highly accurate records may be secured and later enhanced to reveal features the eye alone could not hope to discern. Most visual observers make observational drawings of the Moon's surface. After all, why bother to stand at your scope with pencil and paper when you can use a CCD? Firstly, the essence of astronomy is to observe and there is truly nothing like drawing for developing your observational skills. Secondly, producing a drawing greatly enhances your knowledge of what the subject really looks like. Artistic ability is by no means a prerequisite, the aim is technical accuracy; you don't need to make any sort of artistic statement!

Harold Hill's lunar portfolio is a unique collection of drawings. Astronomical drawing still has an important place alongside photography. Indeed, since astronomical images tend to scintillate because of turbulence in the Earth's atmosphere, drawings constructed by an artist who takes advantage of the fleeting moments of perfect vision are often more detailed than photographs. No one can fail to be impressed by the beauty and artistry of this work and, to the initiated, the accuracy and attention to detail is remarkable.

Unlike traditional drawing as the representation of landscape, still life, etc., the lunar drawing involves some difficulty like weak light or poor seeing that considerably affects the observation. I suggest that you begin finding your way around the Moon by attempting to draw small areas of the lunar surface which lie close to the terminator, the dividing line between the illuminated and dark region of the moon. It is necessary to try and allow yourself around an hour or two for a sketch. Try to identify the feature you are

observing whilst at the eyepiece.

This technique is low cost, only a set of soft-leaded pencils from HB to 5B, an A4 cartridge paper, a brush, and eraser are necessary. Basic outlines are first drawn lightly, using a soft pencil, giving you the chance to erase anything dubious if the need arises. When shading dark areas try to put minimal pressure onto the paper, the darkest areas are ideally shaded in layers. Everything can reach good results, but lot of constancy is required for this technique. Nevertheless I have not reached elevated levels yet even if I have significantly improved my technique. The most important thing to remember is to be patient. Do not rush, even if you are only practising. When the moon is focused in the eyepiece, select and identify just a small target area of the Moon's surface, such as an individual crater, preferably one close to the lunar terminator where most relief detail is visible. I use to sketch the basic outlines on transparent paper, after that I brush the transparent paper with a dust lead, then I make zones of light with a small blade (a razor blade), as visible in Rima Hadley drawing.

To ensure some degree of accuracy in their lunar drawings, many visual observers select a feature to observe in advance of the observing session, and prepare an outline blank showing the main features, based upon a map such as Rükl's *Atlas of the Moon*. Making a general outline blank prior to observing allows the observer to worry about subtle features and attend to detail at the eyepiece instead of expending excessive amounts of time and effort in attaining positional accuracy. Personally, however, I do not like to use this method. It is certainly more interesting to capture the details from an observation in view.

Figure 1: Rima Hadley drawn using the method of the razor blade as for the following images.

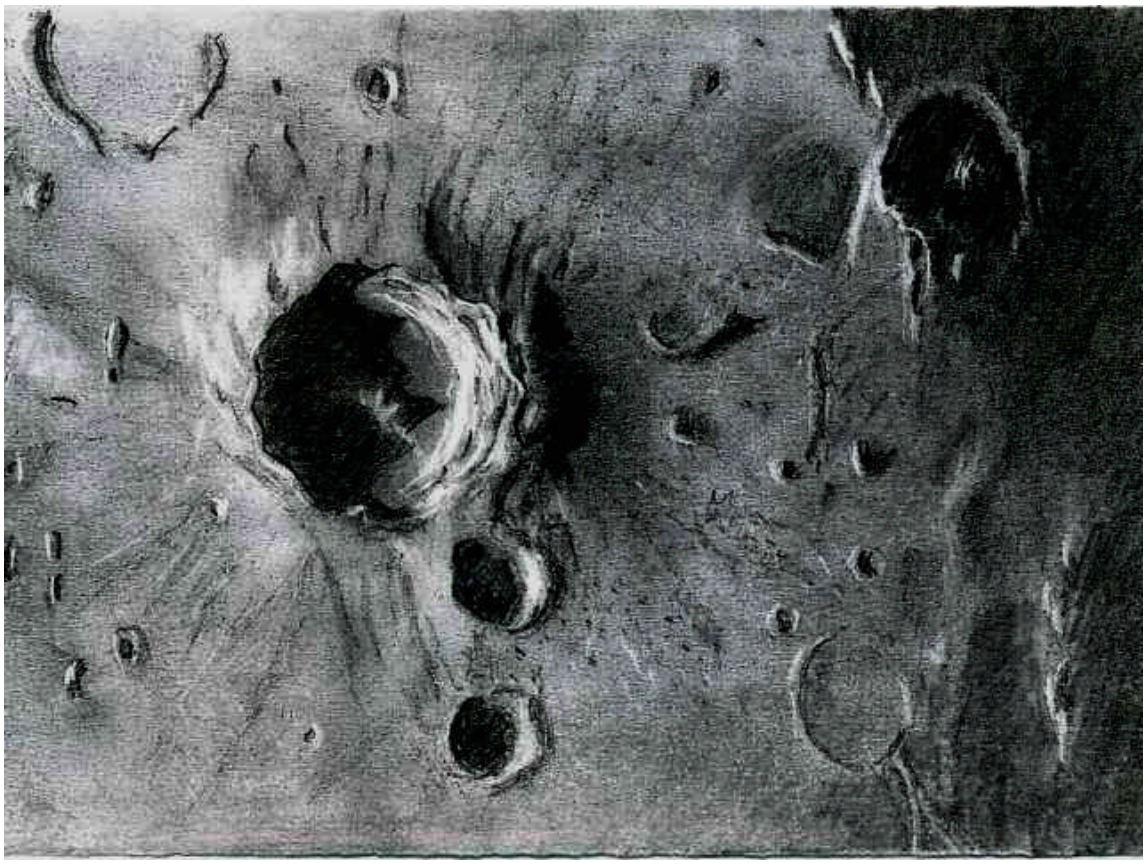

Figure 2: Bullialdus-Gould craters.

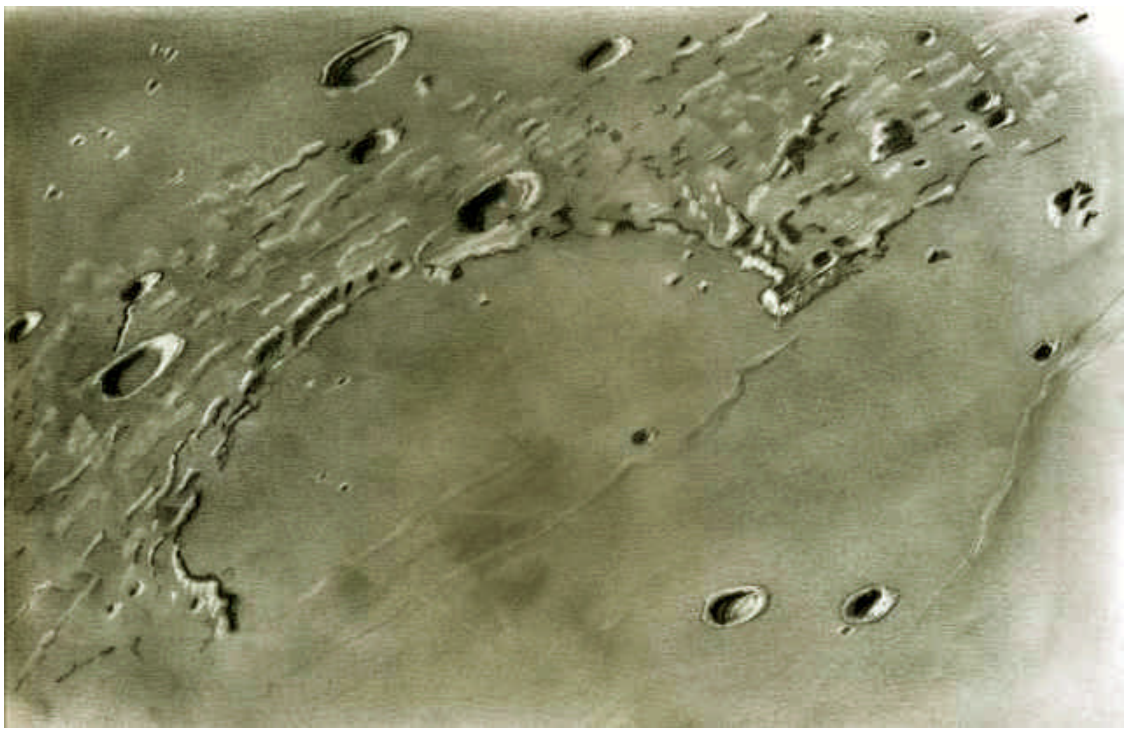

Figure 3: Sinus Iridum.

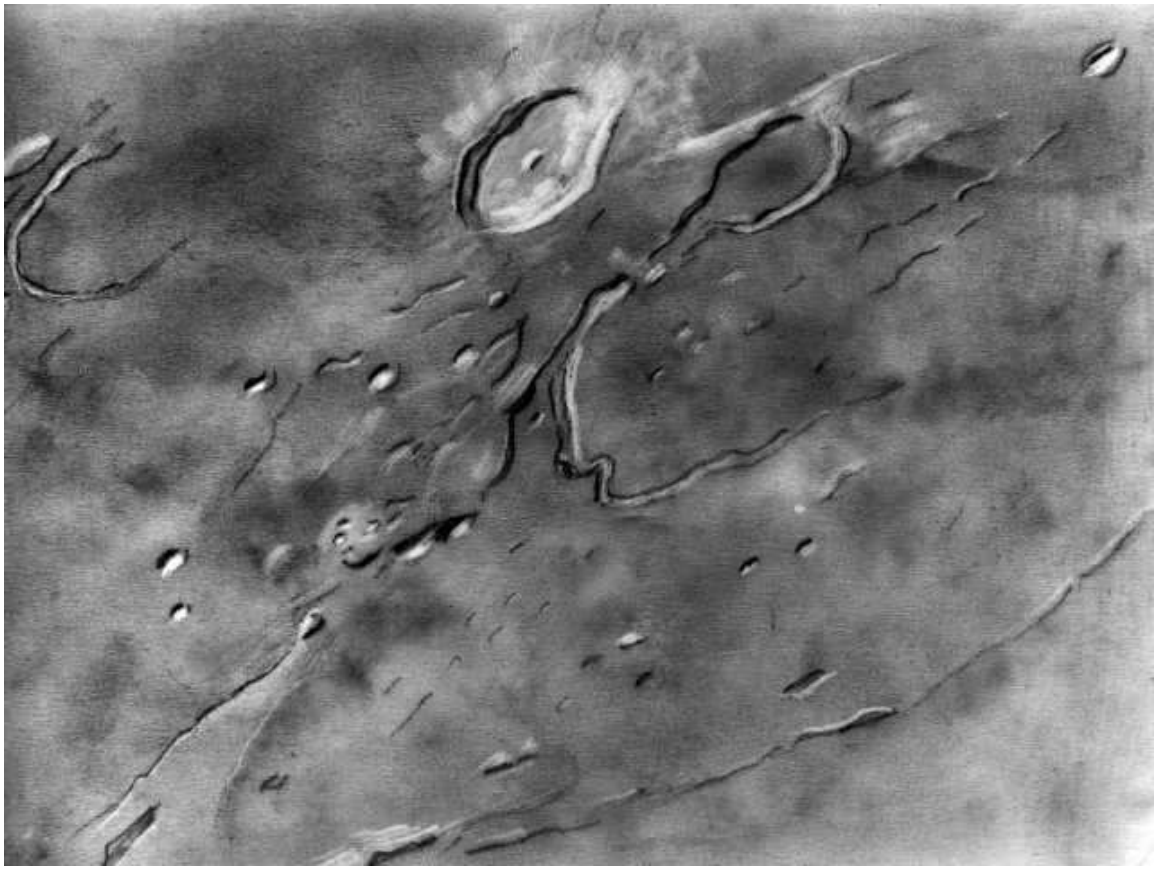

Figure 4: Vallis Schröter.

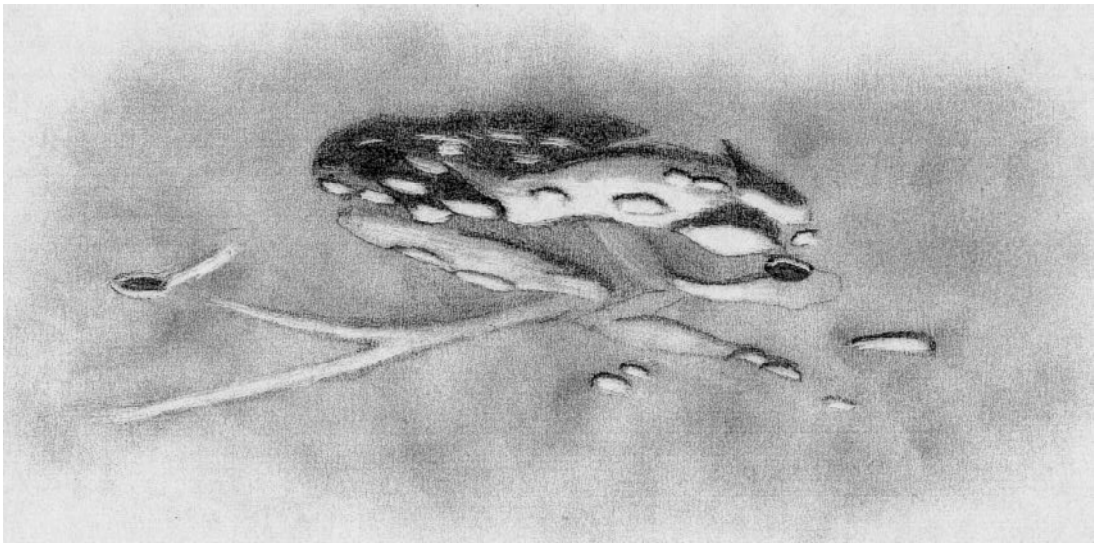

Figure 5: Mons Rümker.

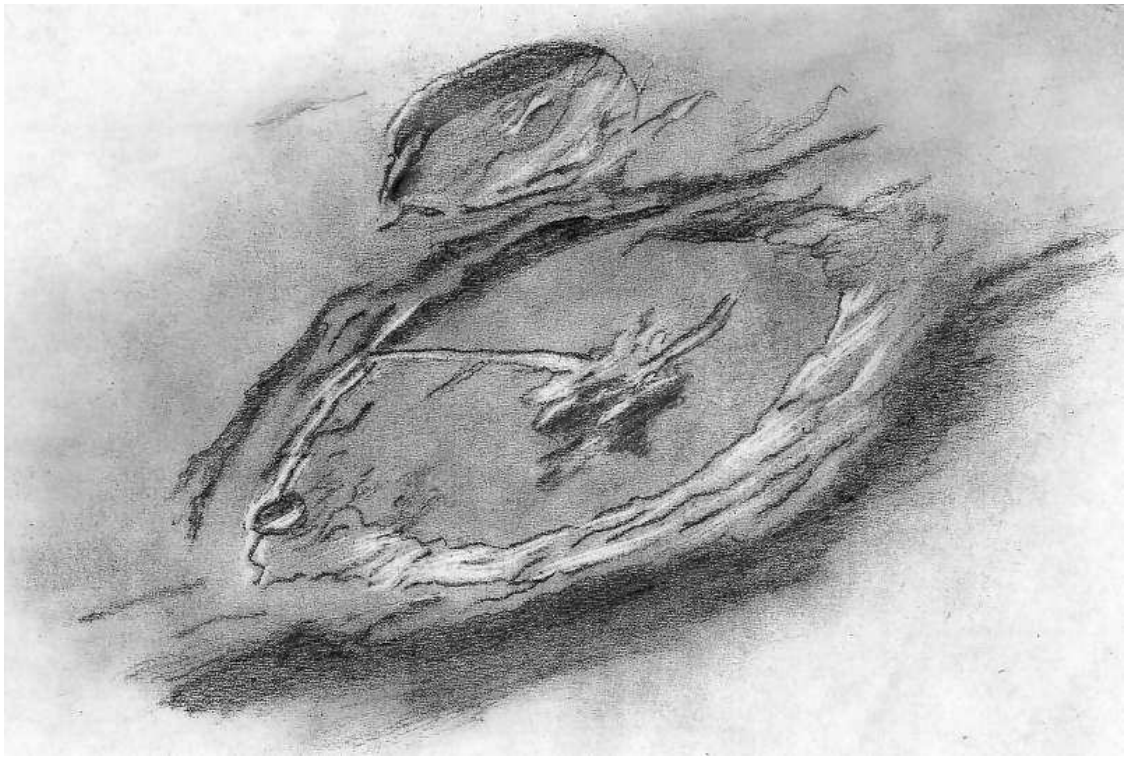

Figure 6: Petavius crater.

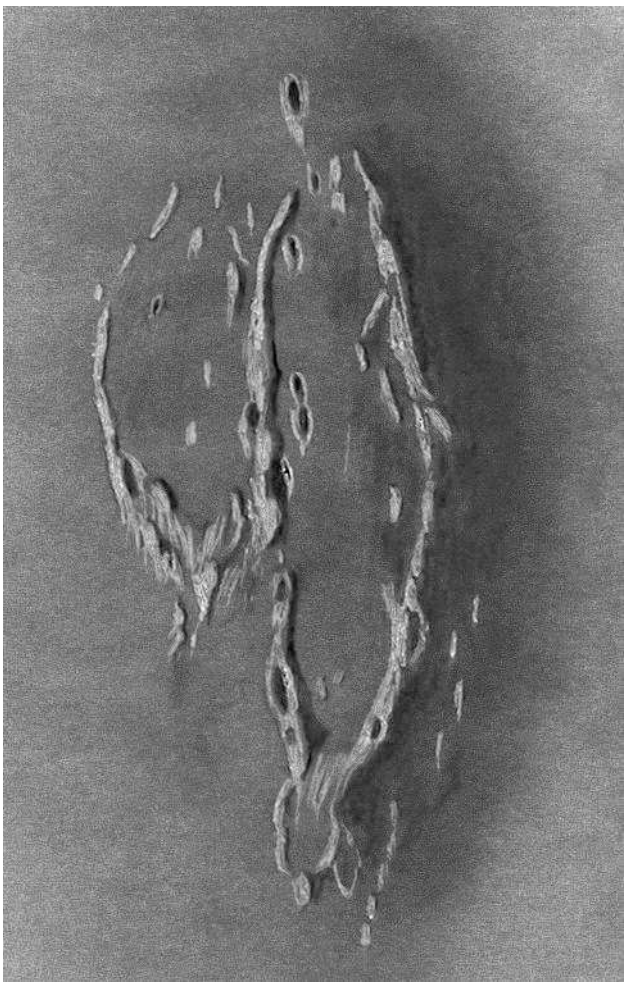

Figure 7: Struve-Russel-Eddington craters.

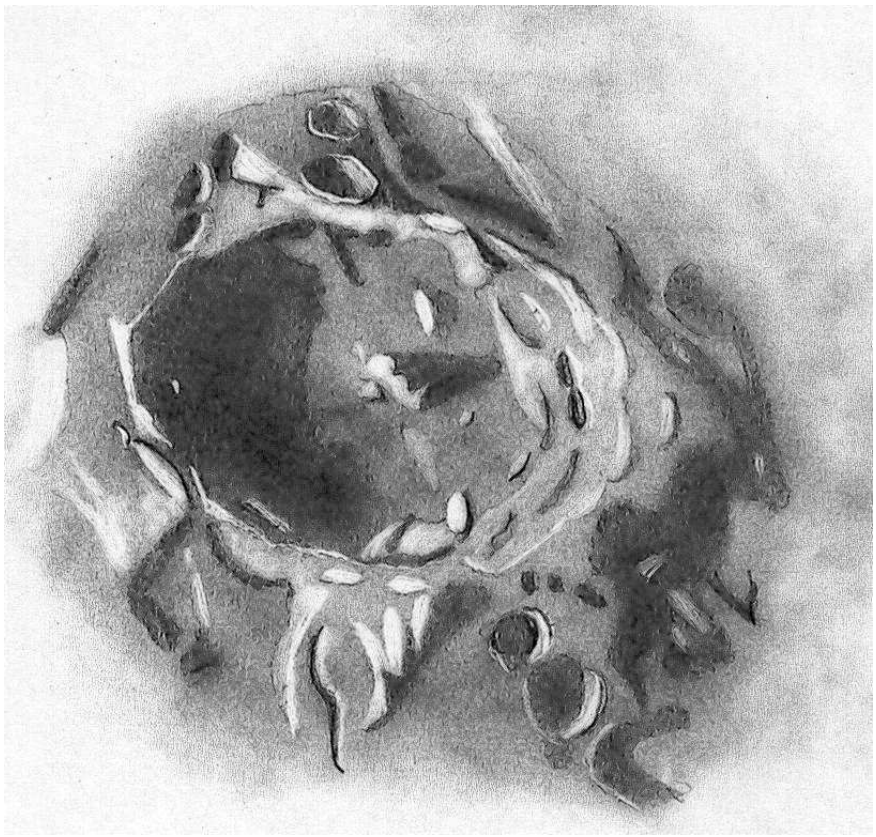

Figure 8: Tycho crater.

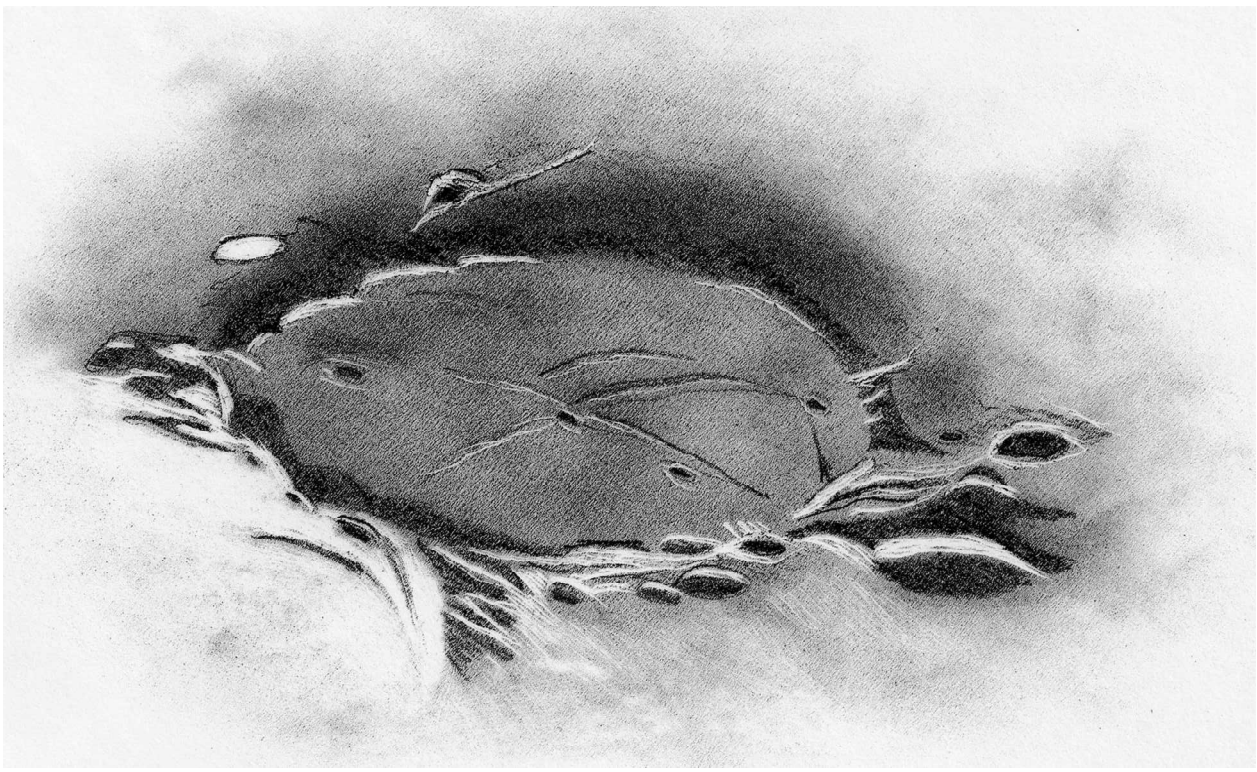

Figure 9: Wargentin crater.

Figure 10: Pythagoras crater.

Figure 11: Rima Hyginus.

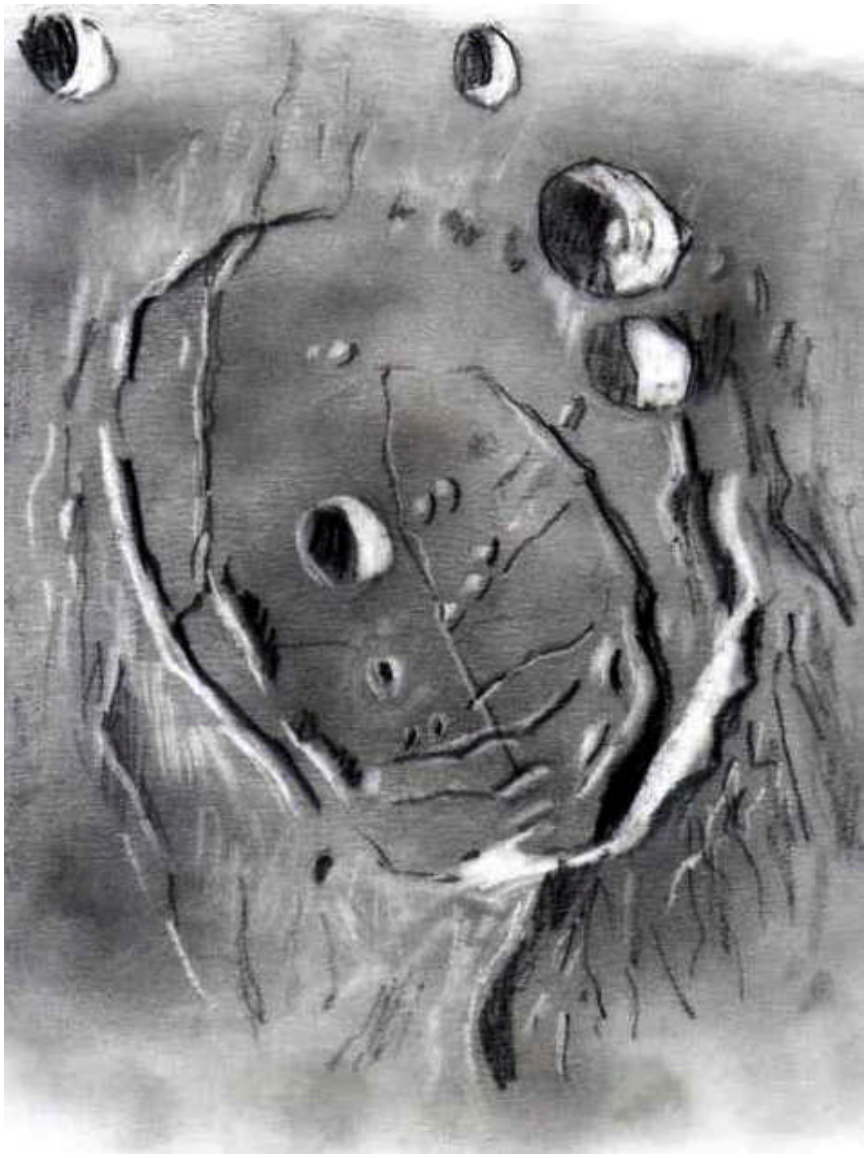

Figure 12: Posidonius crater.

New Atlas of the Moon

Book Review
By Robert A. Garfinkle, FRAS

"New Atlas of the Moon"
By Thierry Legault and Serge Brunier
Translated from the French by Klaus R. Brasch
Firefly Books; 125 pages; $55.00

This outstanding lunar photographic atlas is in a class by itself, and I don't say that lightly. The large format (12-½ x 11-½ inches) allows for the publication of incredibly clear images of the Moon. Thierry Legault took most of the images. The covers are hard, but the book is spiral-bound, which allows the reader to lay the book flat without bending pages at the center of the book. The book contains two main sections; the "Moon from Day to Day", and "Lunar Cartography". The first section is divided by lunation day with a large-scale image for most of the days. One thing that I truly like is that for these large-scale images, they supplied a transparent layover with the feature names on them. Under some of the feature names is the page number where you will find a high-resolution image of the feature and descriptive text about it in the second section. Not all of the features called out on the lunation pages have high-resolution images in the second section. On the text page, the authors give you an image of the Moon as seen on that lunation day as viewed through binoculars (north up) and a larger image as seen through a refractor (south up). A small blurry image shows you what the Moon on that day looks like with the unaided eye. The book contains a clearly written "How to use this Atlas" page that shows typical pages from the book. One is an introduction for a lunation day and pages showing the high-resolution images. A third section, "Lunar Movements" teaches you how the Moon moves around the Earth, covers both lunar and solar eclipses, observe occultations, and gives practical tips for observing the Moon, selecting and purchasing the right kind of telescope and photographic equipment or lunar observing. This section contains minor errors in the way they drew the Sun's rays in their eclipse diagrams. They show the rays as a cone and inverted cone between the Sun and Moon in the solar eclipse drawing and between the Sun and Earth in the lunar eclipse drawing. The Sun's rays are parallel; it is the shadow cast by a sphere that forms a cone pointing away from the light source. Also, the lunar eclipse scale is way off, because they show a series of moons passing through the Earth's shadow taking up almost a quarter of the Moon's orbit. The novice would have no idea that these drawings are not to scale, because that is not indicated. I own a number of lunar atlases and this one is one of the best every produced for use by a beginning lunar observer. The images are downright spectacular and sharp. There are no out-of-focus images, except those previously mentioned. The large format allowed the authors to use large images, which makes it easier for you to see the finer details than what you could see if the images were smaller. When using some of the other lunar atlases that I own, I need a magnifying glass to see these finer details. This is not a problem with this work. The text is clear and informative, and the "how-to-use-this-book" is a big asset. I highly recommend this lunar atlas not only for new lunar observers, but for experienced observers as well.

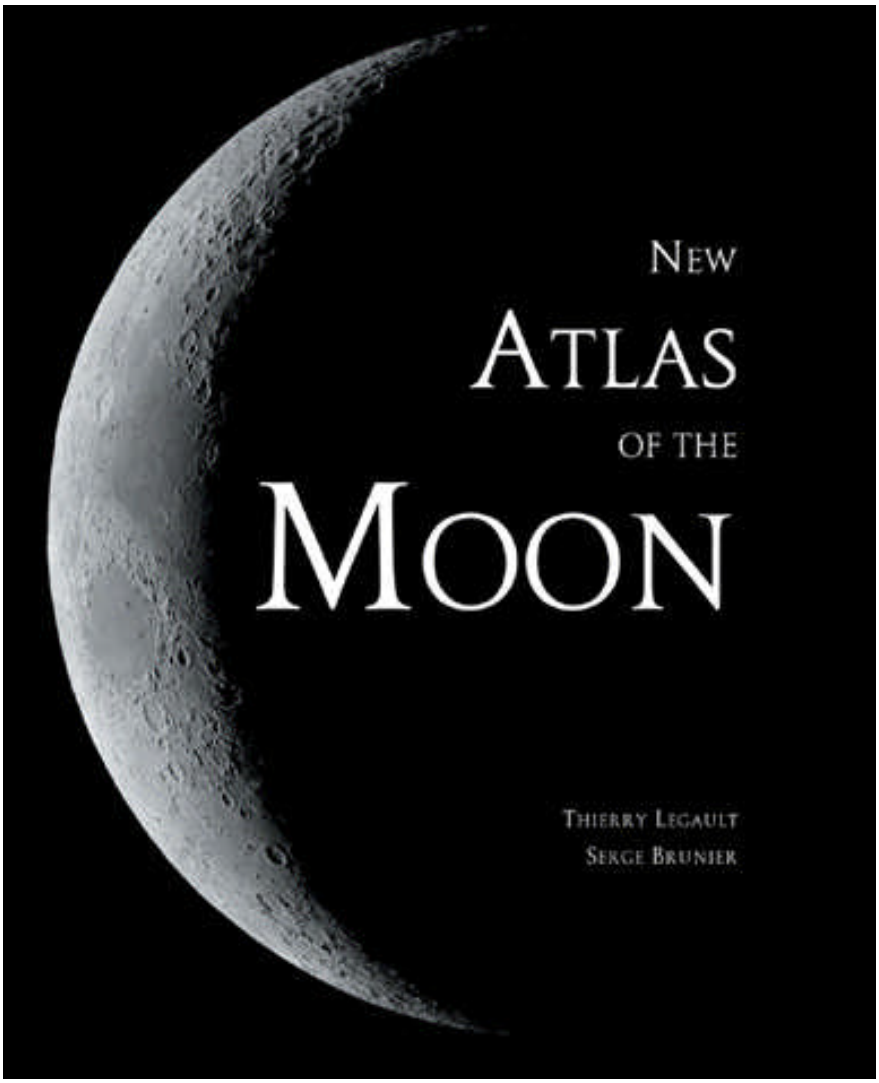

New Atlas of the Moon"
By Thierry Legault and Serge Brunier
Translated from the French by Klaus R. Brasch
Firefly Books; 125 pages; $55.00